Changes driven by the evolution of higher group polarization in the guppy are consistent across different predation pressures and associated with neuroanatomical changes

Alberto Corral-Lopez*[1,2,3,4], Alexander Kotrschal[2,5], Alexander Szorkovszky[6], Maddi Garate-Olaizola[2,4], James Herbert-Read[8,9], Wouter van der Bijl[1], Maksym Romenskyy[10], Hong-Li Zeng[11], Severine Denise Buechel[2,5], Ada Fontrodona-Eslava[2,12], Kristiaan Pelckmans[7], Judith E. Mank[1], Niclas Kolm[2]

*corresponding author: alberto.corral@ebc.uu.se

Affiliations

1 - Department of Zoology and Biodiversity Research Centre, University of British Columbia, Vancouver, Canada
2 - Department of Zoology/Ethology, Stockholm University, Stockholm, Sweden.
3 - Division of Biosciences, University College London, London, United Kingdom
4 – Department of Ecology and Genetics, Uppsala University, Uppsala, Sweden
5- Behavioural Ecology, Wageningen University & Research, Wageningen, Netherlands.
6 - RITMO Centre for Interdisciplinary Studies in Rhythm, Time and Motion, University of Oslo, Oslo, Norway
7 - Department of Physics and Astronomy, Uppsala University, Uppsala, Sweden.
8 - Department of Zoology, University of Cambridge, Cambridge, UK.
9 - Aquatic Ecology, Lund University, Lund, Sweden.
10 - Department of Life Sciences, Imperial College London, London, UK.
11 - School of Science, Nanjing University of Posts and Telecommunications, Nanjing, China.
12 - Centre for Biological Diversity, School of Biology, University of St Andrews, St Andrews, UK

Abstract

One of the most spectacular displays of social behavior is the synchronized movements that many animal groups perform to travel, forage and escape from predators. However, elucidating the neural mechanisms underlying the evolution of collective behaviors, as well as their fitness effects, remains challenging. Here, we study anti-predator behavior in guppies experimentally selected for divergence in polarization, an important behavioral aspect of coordinated movement. We find that groups from artificially selected lines remain more polarized than control groups in the presence of a threat. Neuroanatomical measurements of polarization-selected individuals indicated changes in brain regions previously suggested to be important regulators of perception, fear and attention, and motor response. Additional visual acuity and temporal resolution tests performed in polarization-selected and control individuals indicate that observed differences in anti-predator and schooling behavior should not be attributable to changes in visual perception, but rather are more likely the result of the more efficient relay of sensory input in the brain of polarization-selected fish. Our findings highlight that brain morphology may play a fundamental role in the evolution of coordinated movement and anti-predator behavior.

Introduction

Animals regularly gather - for safety, for exploiting resources, or for mating. Group-living often leads to spectacular forms of collective behavior, and individuals in many taxa coordinate their movements in order to increase efficiency in foraging and travelling, or to confuse predators[1]. Collective motion has evolved multiple times in fishes and is widely understood as a behavioral adaptation aimed at reducing the risk of predation[2]. This behavioral adaptation is underpinned by the efficient acquisition of information from external cues through visual and lateral line sensory systems[3–6]. To date, we have a detailed understanding that coordinated movements in animal groups likely emerge from decision rules that individuals use to interact in groups[e.g. 7,8]. Similarly, correlation-based analyses have revealed how predation levels are associated with variation in collective motion in wild populations (see for instance [9]). Yet, the causes of collective motion are still unclear, particularly how evolutionary changes in collective motion contribute to anti-predator specific situations, or what type of sensory information and information processing schooling fishes use to identify and avoid predators as groups.

The brain, as the central organ controlling locomotion, sensory systems and decision-making, can play an important role in the ability to coordinate movements and decisions made in the context of grouping. As such, variation in the anatomy of the brain could be an important mechanism behind the evolution of collective motion. The link between social factors and changes in multiple brain structures across taxa is well established[10–13], and well-studied in fishes where approximately half of marine and freshwater species come together in groups at different life stages[14]. For instance, a comparative study on Lake Tanganyikan cichlids showed that species with more complex social structures have larger telencephali and hypothalami[15]. These regions are part of the fish forebrain, which has an important function in social behavior[16], and has been associated with social competence in cleaner fish and social orienting in zebrafish[12,17]. In nine-spined stickleback, exposure to larger groups during development is correlated with larger size of the optic tectum, the visual center in the fish brain[18].

Despite its potential importance, empirical studies explicitly testing the association between neuroanatomy and collective motion are to date scarce. Brain regions associated with fish social behavior have also been identified in the few studies explicitly testing the link between neuroanatomy and schooling behavior. Lesion studies in goldfish (*Carassius auratus*) showed that individuals with ablated telencephalon exhibited reduced activity and association with

conspecifics[19]. Also, a study on surface and cavefish populations of *Astyanax mexicanus* living in different light environments showed an underlying positive correlation between optic tectum size and schooling behavior differences between populations[20]. These few previous studies highlight the potential role of neuroanatomy in schooling, as well as the need to account for environmental variation in analyses.

Here we use artificial selection lines of guppies (*Poecilia reticulata*) with divergence in polarization, the degree of alignment of members of a group when swimming. Polarization-selected guppies offer a unique opportunity to empirically evaluate the link between evolution of general schooling behavior, specific anti-predator behavior and neuroanatomy[21]. In relation to many fish species that associate in large schools, guppies have relatively low schooling propensity, with high levels of variation across individuals and across populations as a function of external factors such as predation risk or food availability[22,23]. In our selection lines, intrinsic schooling propensity was increased in female guppies by over 15% compared to controls in just three generations by selecting on individuals that exhibited higher polarization, the level of alignment between individuals moving together in a group[21,24]. Previous assays in the polarization-selected females showed that differences in polarization were caused by the combined effect of the likelihood to align with neighbors' movements, the strength of alignment to larger groups and individual swimming speed[21].

We use these lines to investigate potential changes in the visual system and anti-predator behavior following directional selection for polarization, as well as to study the association between increased schooling propensity and changes in brain anatomy. For this, we performed a series of experiments and measurements to: i) evaluate collective motion patterns and predator inspection of individuals from polarization-selected and control female guppies when swimming in groups, ii) quantify brain region sizes with microcomputed tomography (microCT) of female guppies from polarization-selected and control lines, and iii) perform comprehensive tests of visual capabilities of these fish, spanning eye size, visual acuity and temporal resolution measurements of individual fish. Through the study of collective behavior in an ecologically relevant setting, we identify potential evolutionary pathways for how selection for higher polarization is associated with brain structure size variation.

Results

137

138 **Collective motion in response to predation threat in guppies following artificial selection**

139

140 We investigated whether selection for higher polarization affected cohesiveness and how
141 individuals from groups reacted in response to neighbor movement in a predation context.
142 These behavioral decisions should have major fitness consequences in this species[25].
143 Specifically, we recorded and tracked fish in an experimental arena to obtain positional data
144 and assessed collective motion of groups of eight guppies when exposed to an imminent threat,
145 the presence of an artificial replica of a pike cichlid (*Crenicichla frenata*), a natural predator in
146 wild populations of Trinidadian guppies. Furthermore, we exposed these groups to a non-
147 predator-shaped object to allow for comparisons when presented to a novel object. These
148 assays were performed in combination with open field tests (OFT's) on the same fish groups.
149 In total, we obtained data for 83 polarization-selected groups and 81 control groups of
150 approximately six months of age and of similar body size (polarization-selected: standard
151 length mean [95% CIs] = 24.8 mm [24.0, 25.5]; control: standard length mean = 24.5 mm [23.8,
152 25.3]). Previous analyses of the data for OFT's in these groups provided evidence that selection
153 for polarization altered individuals' speed, how individuals aligned with, and how individuals
154 were attracted towards conspecifics during group motion[21].

155

156 Our analyses of collective motion of female groups exposed to a predator model and a novel
157 object showed predictable results in relation to previous findings observed in OFT's. In the
158 presence of a novel object or a predator model, we observed overall declines of 12% and 17%
159 in the polarization of the groups, while individuals' speed showed 20-fold and 24-fold
160 decreases in the presence of a novel object and a predator model respectively (Supplementary
161 Table 1, Fig. 1A). Previously observed differences between polarization-selected and control
162 groups in these traits were still present in the presence of these stimuli in the experimental arena
163 with approximate differences of 7% (Supplementary Table 2, Fig. 1A). Overall, nearest
164 neighbor distance towards conspecifics in female showed a 10-fold increase in tests with a
165 novel object and with a predator model in relation to OFT's (Supplementary Table 1, Fig. 1A).
166 Such strong reduction in median nearest neighbor distance observed between fish in the
167 presence of these stimuli likely lead to minimum possible values of inter-individual distance in
168 our experimental setup. Indeed, differences between polarization-selected and control lines in
169 nearest neighbor distance observed in OFT's[21] were not present in the presence of a predator
170 model and a novel object (Fig. 1A; Supplementary Table 2). For median speed and group

171 polarization, the predator model elicited a stronger response than the novel object. Specifically,
172 collective motion data showed that guppy groups showed a 4-fold reduction in speed and were
173 4.5% less aligned in the presence of a predator model (LMM_{speed}: $Estimate_{novel\ object\ vs\ predator\ model}$
174 = 3.910 [0.709-7.100], t = 4.71; df = 338; $p < 0.001$; $LMM_{polarization}$: $Estimate_{novel\ object\ vs\ predator}$
175 $_{model}$ = 0.045 [0.022-0.067], t = 2.87; df = 338; p = 0.011: Supplementary Table 1, Fig. 1A).
176
177 **Information processing in response to predation threat**
178
179 *Group polarization spatial patterns*
180 We studied spatial patterns associated with collective motion in our experimental setup by
181 generating heatmaps with average values of group polarization and group centroid within a 20
182 x 20 mm grid for OFT's, predator model and novel object tests performed to polarization-
183 selected and control groups. Visual inspection of heatmaps (Fig. 1B) concords with results
184 obtained from statistical models using summary statistics for each group, suggesting a decline
185 in polarization of the group in the presence of these stimuli. Yet, differences in polarization
186 between control and polarization-selected groups in open field and novel object assays were
187 consistent across all regions of the arena, while the observed differences in assays with a
188 predator model were more pronounced in positions further away from the head of the model
189 (Fig. 1B).
190
191 *Correlation between group polarization and speed*
192 To further characterize potential differences in how information spreads in polarization-
193 selected and control fish groups we assessed the effect of group speed in the alignment of fish
194 when exposed to a predation threat. For this, we generated heatmaps showing the correlation
195 of group speed and group polarization across treatments for our different selection lines (Fig.
196 2). Heatmaps indicated that group polarization of polarization-selected fish in OFTs was
197 constantly close to maximal values of one and differences with control groups were partially
198 independent of the speed of the group (despite larger values of median speed observed in
199 relation to those in control groups). Overall group polarization reduction in the presence of a
200 novel object and a predator model in relation to OFTs were likely associated with a strong
201 reduction in the speed of the group, including periods of no movement of the group. Periods of
202 no movement in response to a threat were observed more frequently in control groups
203 suggesting that they might be an important driver of group polarization differences observed
204 between polarization-selected and control groups. In addition to differences driven by lack of

movement, correlations of group polarization and speed indicated that differences between polarization-selected and control groups observed during collective motion resembling motion in OFT's (mean group speed range 2 – 5 mm/frame) were maintained in the presence of stimuli in the experimental arena (Fig. 2).

Predator inspection behavior

Group polarization spatial patterns and its relationship to swimming speed suggested differences between polarization-selected and control fish in their attention to stimuli presented in the experimental arena. As such, we quantified inspection behavior of individuals in our groups of eight fish in the presence of a predator model. We scored recorded videos for the start and end point for each predator inspection performed by one randomly selected fish in each video. Analyses of predator inspection data showed that females from control lines presented a higher tendency to inspect the predation threat presented in the experimental arena than polarization-selected females. Specifically, we observed that polarization-selected females spent 21% less time inspecting the predator model and the mean duration of predator inspections were 18% shorter in polarization-selected females ($GLMM_{time_inspecting}$: Incidence Rate Ratio (IRR) $_{polarization}$ = 0.79 (0.66-0.95), t = -2.52, p = 0.011; $GLMM_{mean_inspection}$: IRR $_{polarization}$ = 0.82 (0.66-0.96), t = -2.49, p = 0.013, Fig. 2d-e, Supplementary Table 3): We observed a similar trend for total number of predator inspections performed with a 13% reduced frequency of inspections observed in polarization-selected females ($GLMM_{inspections}$: IRR $_{polarization}$ = 0.87 (0.75-1.01), t = -1.85, p = 0.064; Fig. 2c, Supplementary Table 3).

Collective motion during predator inspections

Analysis of positional data and median distance to the stimulus presented in our assays suggested that most inspection behaviors to the predator model were performed during the initial three minutes of the assays (Supplementary Figure 1). Further, the majority of inspections were performed at a range <200 mm and in the tail area of the predator model presented in the experimental arena (Fig. 1A; Fig. 3A). Consequently, we filtered our data to evaluate collective motion patterns of fish groups in the time and locations where predator inspections were performed during our assays (see methods). The overall differences in group polarization found between polarization-selected and control groups were maintained in areas within 200 mm of the predator model (Fig. 3B; $LMM_{polarization< 200mm}$: $Estimate_{selection}$ = -0.044 [-0.088,-0.000], t = -1.984, df = 272, p = 0.048; Supplementary Table 4a-b). Inspection behavior is mainly performed from areas with reduced risk of attack from a predator. In line

239 with such expectation, we found that polarization of all groups was greatly reduced in the area
240 of the predator model tail (Fig. 3B). However, we found no differences in group polarization
241 between selected and control females in the head area of the predator model, but a maintenance
242 of 8% differences in group polarization between polarization-selected and control females in
243 close proximity to the tail of the predator model ($LMM_{polarization - head\ area}$: $Estimate_{selection}$ = -
244 0.037 [-0.102, 0.027], t = -1.53, df = 4.58, p = 0.190; $LMM_{polarization - tail\ area}$: $Estimate_{selection}$ =
245 -0.080 [-0.146, -0.013], t = -1.53, df = -3.48, p = 0.030; Fig. 3B, Supplementary Table 5a-b).
246
247 **Changes in neuroanatomy following artificial selection**
248
249 We used microcomputed tomography (micro-CT) to reconstruct the brain anatomy of 13
250 polarization-selected females, and 15 control females and determine overall brain volume and
251 the volumes of 11 major brain regions that could be safely identified in these brain scans
252 covering the whole brain volume: olfactory bulbs, ventral telencephalon, dorsal telencephalon,
253 thalamus, hypothalamus, nucleus glomerulus, torus semicircularis, optic tectum cup, central
254 optic tectum, cerebellum, and medulla oblongata (see methods). We next used this data set to
255 evaluate potential associations between collective behavior and neuroanatomy. Polarization-
256 selected and control fish showed no differences in relative brain size (whole brain volume in
257 relation to their body size; $LMM_{relativebrain}$: t = -0.41, df = 23.29, p = 0.682; Fig. 4a). However,
258 analyses of relative brain region size (volume of each region in relation to the volume of the
259 rest of the brain) indicated that the thalamus and optic tectum cups are approximately 7% and
260 4% larger in polarization-selected than control females respectively ($LMM_{thalamus}$: Odds Ratio
261 (OR) $_{polarization}$ = 0.929 (0.866-0.998); t = 2.187, df = 25, p = 0.038; $LMM_{o.tectum}$: Odds Ratio
262 (OR) $_{polarization}$ = 0.959 (0.924-0.994); t = 2.409, df = 23.09, p = 0.024; Fig. 4a), and the medulla
263 oblongata is an 8% larger in control females ($LMM_{medulla}$: Odds Ratio (OR) $_{polarization}$ =1.08
264 (1.01-1.14); t = -2.65, df = 23.91, p = 0.013; Fig. 4a). All other eight brain regions measured
265 presented no differences between polarization-selected and control females in relative region
266 volumes (Fig. 4a-b, Supplementary Table 6).
267
268 In parallel, we analyzed brain region volume differences using a more conservative approach
269 and found similar and consistent differences between selection lines. Specifically, we used a
270 multivariate Bayesian model that included the relative size of the 11 brain regions as dependent
271 variables. Posterior samples drawn from the multivariate model indicated that confidence
272 intervals for the difference in relative volume in the medulla oblongata, the optic tectum cups

273 and the thalamus between polarization-selected and control females did not overlap with zero
274 (Supplementary Table 7a).
275
276 We then used the multivariate Bayesian model to evaluate the correlation in relative brain
277 region volume between multiple regions measured. We focused on evaluating correlations with
278 other brain regions for the three regions significantly differentiated between lines following
279 artificial selection (Supplementary Table 7b). We found no correlation between optic tectum
280 cup relative volume and volume of any other region measured. However, we found a significant
281 inverse correlation between thalamus and medulla relative volume ($rescorr_{Medulla\text{-}Thalamus}$ [95%
282 CIs]: -0.40 [-0.65 / -0.12]). This finding suggests that the opposite differences observed in the
283 volume of these two brain regions between control and polarization-selected female guppies
284 may be linked to changes in brain development processes associated with artificial selection
285 for higher coordinated motion.
286
287 **Information acquisition through the visual system**
288 Efficiently acquiring information through the sensory system, mainly through visual cues, is a
289 basic principle of collective motion in shoaling fishes[3]. Given observed differences in the size
290 of the optic tectum cups between polarization-selected and control fish, we investigated
291 potential differences in visual perception between lines. For this, we compared eye size and
292 two key characteristics of the visual system to track movement of conspecifics, visual acuity
293 and temporal resolution.
294
295 *Eye size*
296 We quantified eye size in females from polarization-selected (n = 57, standard length mean
297 [95% CIs] = 27.0 mm [26.6, 27.4]) and control lines (n = 55, standard length mean [95% CIs]
298 = 27.1mm [26.8, 27.5]). Eye size is a common indicator of visual capacities of organisms[26],
299 and comparative studies across fish species suggest that larger eyes correlate with improved
300 visual abilities[27]. In our study, we found no difference between polarization-selected and
301 control lines in either absolute eye size or relative eye size, the proportional size of the eye in
302 relation to body size (Fig. 5A; $LMM_{eye\ size}$: $Estimate_{selection}$ = -0.03 [-0.24, 0.19], t = -0.52, df =
303 2, p = 0.66; $LMM_{relative\ eye\ size}$: $Estimate_{selection}$ = -0.00 [-0.01, 0.01], t = -0.13, df = 2, p = 0.90;
304 Supplementary Table 8). As previously reported in guppies[28] ,we found a strong positive
305 correlation between eye size and body size (Pearson's correlation test: t = 11.72, df = 110, p <
306 0.001, cor [95% CIs] = 0.74 [0.65, 0.82]), but this correlation did not differ between

307 polarization-selected and control lines ($LMM_{eye\ size}$: $Estimate_{selection*body\ size}$ = 0.010 [-0.016,
308 0.039], t = 0.75, df = 101, p = 0.45).
309
310 *Visual acuity*
311 We further assessed potential differences in visual perception between selection and control
312 lines by quantifying visual acuity in the same individuals for which eye size was measured.
313 Visual acuity allows an individual to resolve spatial detail and can be critical for an organism's
314 fitness[29]. We measured visual acuity in our fish by quantifying their innate optomotor response
315 in contrasting rotating gratings. This a widely used method to study visual acuity in multiple
316 fish species, including guppies[30–32], and we have previously used this approach to evaluate the
317 visual system of guppies in similar contexts[28,33]. Following the methods in ([28]), we exposed our
318 fish to a series of six stimuli with rotating and static gratings of different widths at the lower
319 end of the known guppy visual acuity, where thinner widths are more difficult to perceive. If
320 polarization-selected and control groups differed in their ability to resolve spatial ability,
321 differences in their optomotor response towards these rotating stimuli at the lower end of the
322 guppy visual acuity should be expected. However, we found no difference in their average
323 optomotor response combining data from all stimuli (LMM_{acuity}: $Estimate_{selection}$ = 0.00 [-0.08,
324 0.009], t = 0.11, df = 12.88, p = 0.913; Supplementary Table S9a), or in analyses independently
325 evaluating specific optomotor response for any of the six stimuli presented (Fig. 5B;
326 Supplementary Table 9c).
327
328 *Visual resolution tracking movement*
329 Although the ability to resolve spatial detail, acuity, is arguably an important visual parameter
330 for guppies to recognize conspecific positions in shoals, it provides no information on an
331 individual's ability to track movement[34]. Similar to many social fish species, guppies swim
332 with a saltatory movement style that features discrete changes in speed and direction[9].
333 Consequently, we implemented an additional experiment that evaluated potential differences
334 between polarization-selected and control fish in their temporal assessment of speed and
335 direction changes. Using the same experimental apparatus used to evaluate visual acuity, we
336 video recorded female guppies from our selection and control lines and exposed them to a
337 single-width rotating stimulus that moved in multiple directions and at different speeds (see
338 methods). We next used automated tracking to obtain orientation and speed of the fish for each
339 frame and to quantify their direction and speed in relation to the stimuli presented at each time
340 point. If polarization-selected and control groups differed in their ability to track movement,

differences in the time following the correct direction of the stimuli and the deviation of their speed in relation to the stimulus speed should be expected.

Overall, fish followed the correct direction of the rotating stimulus for a significant proportion of the time. This was the case when the stimuli were presented in both a clockwise direction an in counterclockwise direction (Supplementary Figure 2, Supplementary Table 10). Overall, swimming speed did not significantly deviate from the stimuli rotating speed at the two lowest speed levels (Supplementary Figure 2, Supplementary Table 10), but was less than the stimuli speed at the two highest speed levels (Supplementary Figure 2, Supplementary Table 10). This was true for both directions in which stimuli were presented, but the mismatch between swimming and stimuli rotation speed was greater at the higher speed when the stimulus rotated anticlockwise (Supplementary Figure 2, Supplementary Table 10).

We compared the performance of polarization-selected and control fish in the test to evaluate their visual temporal resolution while shoaling. We found no differences between polarization-selected and control lines in their deviation of their swimming speed in relation to the stimuli rotating speed for their combined scores across speeds and direction of rotation (Fig. 5C; $LMM_{speed\ deviation}$: $Estimate_{selection}$ = -0.46 [-8.74, 7.83], t = -0.46, df = 2.64, p = 0.863; Supplementary Table 10a), or for their speed observed at any particular speed at direction of rotation (Supplementary Figure 2, Supplementary Table 10a). Similarly, polarization-selected and control females spent similar proportions of time following the stimuli during changes in stimuli rotating speed (Supplementary Figure 2; Supplementary Table 10a; $LMM_{proportion\ time}$: $Estimate_{selection}$ = 0.00 [-0.14, 0.15], t = 0.10, df = 2.52, p = 0.928).

Discussion

Our work demonstrates that selection for schooling behavior in female guppies has important implications for how this species behaves in the presence of potential threat. Analyses of motion patterns in these fish show that polarization-selected groups maintain higher polarization and speed when exposed to a potential threat. In addition, our analyses indicate that individuals from polarization-selected groups spend less time inspecting the threat than individuals from control lines. We further studied visual capacities in these fish and find no differences between polarization-selected and control individuals in visual acuity, temporal resolution or eye size, suggesting that effective processing of visual information in the brain is

key for the observed differences in their ability to synchronize their swimming with close neighbors at multiple contexts.

In parallel, our results suggest that artificial selection for higher polarization has produced significant changes in the brain anatomy of female guppies. Neuroanatomical measurements indicate that polarization-selected fish exhibit a larger thalamus and a large optic tectum cup, but a smaller medulla oblongata, compared to control fish. These rapid changes in brain region sizes in response to selection for polarization behavior are consistent with previous artificial selection directly on neuroanatomy, which resulted in rapid shifts in both relative brain size and relative telencephalon size, in just a few generations in guppies[35,36].

Below, we discuss the implications of these discoveries for our understanding on how the association between brain morphology and anti-predator behavior might drive the evolution of collective behavior.

Information processing in a predation threat context

Speed plays a prominent role in structuring fish schools, as individuals adjust their distance and alignment with neighbours through changes in speed[21,37,38]. Indeed, empirical studies across several species, as well as modelling approaches, have recently demonstrated a positive correlation between individual's speed and group polarization[38–43]. In our experiments, the presence of a novel object and a predator model prompted strong reductions in the median speed of individuals in the test. Yet, similar differences between polarization-selected and control females in individual's median speed and polarization were maintained across all contexts. Swimming performance tests previously performed in these fish demonstrated that selection did not target fish with better physiological capacities to swim faster, but those showing higher speed in response to neighbor positions[21]. Taken together, our results from these selection lines suggest that selection for coordinated movement is largely mediated by individuals' speed, and that group coordination characteristics such as polarization can emerge from individuals' tendencies to group with conspecifics and fitness benefits acquired from such tendencies at specific contexts.

Schooling in fishes is widely understood as a behavioral adaptation to escape the effect of predation[1]. These synchronized movements have been shown to confer two major benefits to schools, facilitating escape through transfer of information from closer neighbors[44], or by

confusing the predator in which individual to attack[45]. The use of a static predator model in our assays does not allow us to infer any potential benefit of higher polarization on the confusion effect towards predators. However, our results show that directional selection and associated changes in the brain are correlated to behavioral changes in the presence of a threat and that it might affect individual ability to acquire private information about a potential predator. The reduced time spent inspecting the predator model by polarization-selected females, coupled with the fact that polarization-selected groups remained more polarized closer to the predator model, especially around the tail of the predator, suggest this a likely possibility. However, further comparisons within asocial and social contexts should be implemented to disregard the alternative explanation that directional selection leads to changes in predator inspection behavior also when fish have no access to social information.

Our study only measured fitness effects indirectly, using a predator model. Yet, previous work demonstrated that shorter inspection times towards the same predator models are associated with higher survival in the species[46,47]. Experiments with virtual prey analyses have also shown that individuals in groups with higher polarization are at lower risk of predation[45]. As such, our results following directional selection for polarization are consistent with the idea that selection acting on how individuals interact during motion might confer important fitness benefits for individuals showing higher coordination with conspecifics and reinforced in specific contexts, such as high-predation environments. Yet, such benefits might trade-off with a reduced level of private information obtained by individuals in relation to potential threats or foraging sources. In sticklebacks less sociable individuals are more likely to discover food first in a foraging context[37]. This agrees with our results in experiments with a predator model, where faster individuals' speed and higher tendencies to group with conspecifics seem to drive the observed lower time inspecting the predator model in the arena and acquire private information on a potential threat. Overall, these factors are arguably important selective pressures in natural populations where guppies from high predation habitats swim with higher coordination and in larger groups[39,48]. Indeed, guppies from higher predation populations have been shown to rely less on private information for foraging resources, than those from lower predation populations[49]. Further studies evaluating fitness effects of relying in social versus private information across different predation pressures is paramount to understand how anti-predator behavior and collective motion drive evolutionary patterns at the proximate level.

Brain morphology and collective behavior

We found two brain regions that were larger in relation to the rest of the brain in polarization-selected fish, the optic tectum cup and the thalamus. The optic tectum is the terminus of a vast majority of optic nerve fibers and axons of retinal cells[50] and as such is the primary vertebrate visual center. Despite wide variation in optic tectum size across teleost species, this region is known to control eyes and head movement in fish, as well as forming instant representations of the immediate surroundings to transform visual cues into behavioral responses[50,51]. This function is primarily achieved in superficial layers of the tectum[52], which corresponds to the optic tectum cup region used in our neuroanatomical parcellation of major brain regions in the guppy[53].

The evolved differences in optic tectum cup size between polarization-selected and control female guppies we found are concordant with phenotypic plasticity findings in nine-spined stickleback where it was found that individuals reared in groups developed larger optic tectum that those reared individually[18]. Differences in the ability to acquire sensory input have previously been associated with differences in schooling propensity[54]. In our experiment, rapid evolution of higher polarization did not lead to changes in visual performance or eye size. Together, these findings suggest that differences found between polarization-selected and control lines in this section of the optic tectum should have an effect in their ability to control body orientation during complex social maneuvers such as predator evasion and swimming with low inter-individual distances, but not in sensory information acquisition. This is consistent with current considerations of the tectum as more than a visuomotor relay, with implementation of intrinsic processing of visual information to extract critical features and send processed outputs to the posterior thalamus and then to further decision-making regions of the brain[51].

The primary receiving region of processed inputs from the tectum, the thalamus, was also found to be enlarged in polarization-selected females. To date, the level of homology between the mammalian and teleost thalamic regions is under strong debate[55,56]. In mammals, the thalamus plays critical roles in the modification, filtering and distribution of sensory and mechanosensory information into decision-making regions of the brain[56,57]. Recent findings in zebrafish suggest that these tasks are performed mainly by the preglomerular complex, whose developmental origin might be outside the diencephalic area that contains the thalamus in mammals[58]. The neuroanatomical atlas we created to analyze relative region size does not

allow us to assess whether this particular region is part of the thalamus area which has been enlarged in polarization-selected females. However, our results of strong gene expression changes in the telencephalon of polarization-selected and control females in response to decision-making across social contexts[59], are in agreement with a higher efficiency in the relay of processed information towards the telencephalon, potentially facilitated by an enlarged thalamus. Studies across teleosts and mammals do agree on that the thalamus have an important role in the development of glutamatergic and GABAergic relay nuclei, with crucial roles in neurotransmission and inhibition. Interestingly, functional characterization of genomic and transcriptomic analyses performed in these selection lines identified a crucial role of glutamatergic synaptic function in the evolution of schooling[59]. Taken together, our results suggest that changes in the development of glutamatergic relay nuclei driven by a larger thalamus might affect the ability of individuals to synchronize their movements in a shoal. In parallel, and while not directly addressed in this study, the regulatory role of the thalamus in aggressiveness is concordant with common expectations of lower aggression levels in group-living species ([reviewed in 60]). As such, further quantifications of the anatomical characteristics of the thalamus in relation to aggression levels within and across species might be a promising avenue for future research.

In contrast to the thalamus and the optic tectum cup, we found that the medulla oblongata was smaller in polarization-selected lines. The medulla oblongata is an important relay center of nervous signals between the spinal cord and ascendant brain regions with well-described functions in teleosts. First, it has an important role in basic motor function through processing of mechanosensory stimuli from hydrodynamic information[61]. Consistently found across fish species, the lateral line nerves terminate in the medial and caudal octavo lateralis nucleus in the medulla[62]. As the lateral line is crucial for schooling through cues that allow fishes to assess neighbor changes in speed and direction, the reduced relative size of the medulla in polarization-selected lines could be associated with potential differences in the ability to integrate and process information received through these nerves. Yet, our previous studies evaluating motor control capabilities found no difference between polarization-selected and control female guppies[21,63]. Further studies evaluating information processing of mechanosensory input in these selection lines is nonetheless paramount, with special focus on low light and high turbidity conditions.

510 Finally, studies in fishes indicate that the medulla has an important role for processing
511 somatosensory signals, with special emphasis in auditory and gustatory signals[64,65].
512 Specifically, the vagal lobe, part of the medulla, is described to have a prominent role in
513 processing taste. Consistent with our results, the vagal lobe of larval reef fishes is larger in
514 solitary as compared to more social species[66]. While not tested in this study, it may be that the
515 reduction in medulla observed in polarization-selected lines might be associated with important
516 changes in the auditory system and the ability to perceive different tastes. In line with this
517 reduction in the size of the medulla oblongata, our results show that three other brain regions
518 have significant hypoallometric relationships with the medulla (see Supplementary Table 4b):
519 the cerebellum (motor control center), the thalamus and the hypothalamus (hormonal
520 regulation center). Gene expression of *angiopoietin*-1, a locus implicated in brain tissue
521 development, showed contrasting expression levels between the medulla and the thalamic and
522 hypothalamic regions[67]. Based on this, we hypothesize that selection for more coordinated
523 motion leads to a trade-off between general sensory capabilities that are not important in
524 coordinated movements and specific sensory capabilities required to coordinate movement
525 with neighbors. In the future, it will be interesting to investigate the association between
526 schooling propensity, brain anatomy and potential trade-offs between sensory and
527 mechanosensory capacities.
528

529 ## Conclusion

530

531 Our empirical approach with behavioral assays on artificial selection lines with divergence in
532 polarization show that collective motion differences are consistent in the presence of a predator
533 threat and that predator inspection behavior varies between the selection lines and the control
534 lines. Moreover, we reveal differences in neuroanatomy that could provide a mechanistic
535 explanation to the observed behavioral differences. Based on our discoveries, we propose that
536 changes in behavior are intimately intertwined with matching changes in brain morphology
537 during the evolution of collective behavior.
538

539 ## Methods

540

541 **<u>Artificial selection for higher group polarization</u>**

542

543 We evaluated the association between brain anatomy and collective motion in female guppies
544 following artificial selection for higher polarization. Extensive detail on the selection procedure
545 can be found in ([21]). In short, groups of female guppies were tested in repeated open field tests
546 and sorted in relation to the mean polarization of the group, the degree to which the individuals
547 of a group move with higher alignment[21,24,68]. For three generations, females from groups with
548 higher polarization were bred with males from those cohorts to generate three up-selected
549 polarization lines. In parallel, random females were exposed to the same experimental
550 conditions and bred with unselected males to generate three control lines. Third generation
551 polarization-selected females presented on average a 15% higher polarization, 26% higher
552 median speed and 10% higher group cohesiveness (i.e. 10% shorter nearest neighbor distances)
553 in comparison to control females[21]. Further tests in these lines showed that selection for higher
554 directional coordination was not only driven for selection for faster moving fish. This is
555 because polarization-selected lines were still 5.7% more polarized after statistically controlling
556 for speed differences, and the distance to conspecifics was an important factor driving
557 differences in speed between polarization-selected and control lines[21]. The selection procedure
558 targeted polarization on female groups and we found a weaker response to selection in males,
559 and therefore subsequent neuroanatomical, behavioral and physiological studies focused on
560 females. All fish were removed from their parental tanks after birth, separated by sex at the
561 first onset of sexual maturation, and afterwards transferred to single-sex groups of eight
562 individuals in seven liter tanks. We kept all fish used for anti-predator response experiments,
563 visual capacity tests and brain morphology measurements in these groups throughout their life
564 span. Fish were not reused for experiments across these three categories. All tanks contained 2
565 cm of gravel with continuously aerated water, a biological filter, and plants for environmental
566 enrichment. We allowed for visual contact between the tanks. The laboratory was maintained
567 at 26°C with a 12-h light:12-h dark schedule. Fish were fed a diet of flake food and freshly
568 hatched brine shrimp daily.
569
570 **Anti-predator response in guppies following artificial selection**
571
572 *Collective motion*
573 We evaluated anti-predator behavior in polarization-selected and control female guppies by
574 conducting assays on 164 groups of eight fish in white arenas with 55 cm diameter and 3 cm
575 water depth (polarization-selected: n = 83, standard length mean [95% CIs] = 24.8 mm [24.0,
576 25.5]); control: n = 81, standard length mean [95% CIs] =24.5 mm [23.8, 25.3]). Each group

577 was initially assessed in an open field assay in the arena for ten minutes, and collective motion
578 data from these open field assays was previously used to analyze differences in social
579 interactions[21]. After ten minutes, we sequentially introduced a novel object and a predator
580 model for 6-minute periods in the centre of the experimental arena. In half the assays, we
581 introduced the novel object first and the predator model second, with the order reversed in the
582 other half of the assays. We used a blue coffee mug as a novel object and a fishing lure (18 x
583 3 cm) custom-painted to resemble the pike cichlid Crenicichla frenata, a natural predator on
584 the guppy, as the predator model. These objects have been previously used to successfully
585 reproduce natural behaviors of the guppy in response to a novel object and a predation threat[47].
586 To facilitate automated data collection, the position and orientation of the predator model was
587 kept constant by using magnets in the bottom of the fishing lure and in the central position of
588 the experimental arena. We provided external illumination to avoid shadowed areas in the
589 circular arena. Disturbances were minimized by performing all assays in an isolated room of
590 the laboratory. Under these conditions the presence of stimuli should be a major driver of the
591 spatial locations of fish in the experimental arena. However, we are unable to quantify the
592 effect of arbitrary spatial preferences in our results. Prior to the start of the assay, the eight-fish
593 group was confined in the centre of the arena for two minutes in an opaque white 15 cm PVC
594 cylinder. After this acclimation period, we lifted the cylinder and filmed the arena using a Point
595 Grey Grasshopper 3 camera (FLIR Systems; resolution, 2048 pixels by 2048 pixels; frame rate,
596 25 Hz).
597
598 We tracked the movement of fish groups in the collected video recordings using idTracker[69]
599 and used fine-grained tracking data to calculate speed, polarization and nearest neighbor
600 distance in Matlab 2020 following methods established in ([70]). For speed, we obtained the
601 median speed across all group members by calculating the first derivatives of the x and y time
602 series, then smoothed using a third-order Savitzky–Golay filter. For nearest neighbor
603 distance, we obtained the median distance to the nearest neighbor for every fish across all
604 frames. For group polarization, we calculated the median global alignment, which indicates
605 the angular alignment of all fish in the arena. Calculations of median global alignment in each
606 frame were only calculated if six out of the eight members of the group presented tracks
607 following the optimization of our tracking protocol in the setup in ([24]). No differences
608 between completeness of tracks were observed between polarization-selected and control
609 groups for any of the treatments in our experiment (Supplementary Figure 3). For all
610 measurements trials with less than 70% complete tracks were disregarded for further

611 analyses. We additionally used R (v4.1.3), RStudio (v2022.07.0) and the tidyverse package[71–
612 73] to generate heatmaps with average values of group polarization and group centroid within
613 20 x 20 mm grid cells for each frame (Fig. 1B). To avoid biases in group centroid
614 measurements potentially resulting from single individuals or small subgroups at large
615 distances, we limited the analyses to frames in which at least six individuals formed a
616 connected group, with an interindividual distance of 10cm counting as a connection. Grid
617 cells that did not contain values for a minimum of 8 groups per treatment were disregarded.
618 No differences between the proportion of frames used were observed between polarization-
619 selected and control groups for any of the treatments (Supplementary Figure 3). To evenly
620 compare motion patterns when presented with a novel object and a predator model to those
621 obtained during the open field assays, we limited our analysis of the open field assay data to
622 the initial six minutes of the recording.
623
624 We used LMMs with median speed, polarization and nearest neighbor distance as dependent
625 variables to test for potential differences between polarization-selected and control lines.
626 Selection regime, the type of stimulus presented and the interaction between these two were
627 included as fixed effects, and body size of fish was coded as a covariate, with a random
628 intercept for each replicated selection line and the order of presentation of stimuli as random
629 factors. All models were run in R (v4.1.3) and RStudio (v2022.07.0)[71,73] using lme4 and
630 lmerTest packages[74,75]. Model diagnostics showed that residual distributions were roughly
631 normal with no evidence of heteroscedasticity. We obtained post-hoc comparisons of the
632 response between selection line regimes at different levels of other fixed effects in the previous
633 models using the emmeans package[76] with the tukey-adjustment method for multiple
634 comparisons.
635
636 *Predator inspection behavior*
637 ***Behavioral scoring.*** Positional data and analyses of median distance to center in our data
638 indicated that groups of fish swam closer to the stimuli presented in the initial minutes
639 following the addition of a predator model in the experimental arena, when compared to the
640 same time periods following the addition of a novel object (Fig. 1A; Fig. 3A; Supplementary
641 Figure 1). This observation matched previous findings in similar experiments performed on
642 guppies[47] and likely corresponds to the stereotypical behavioral response of guppies to inspect
643 and gain information of a potential threat[25]. A predator inspection in guppies is characterized
644 by an approach to the predator, monitoring predator activity and swimming sideways with an

645 arched body. Based on this information, we manually visualized the videos during the first
646 three minutes after addition of the predator model and scored the behavior of one randomly
647 selected fish in the group using BORIS[77]. While blind to the selection line treatment, the start
648 and end time of each predator inspection performed by the focal fish was scored for each
649 video. We used the start and end time of predator inspections to calculate the number of
650 inspections, average inspection duration and the total time that was spent inspecting per fish.
651 Next, we fit a statistical model for each variable as a dependent variable using a zero-inflated
652 beta distribution and a logit link function for the conditional mean in the package glmmTMb[78].
653 We used the selection line regime as a fixed effect. A random intercept for each replicated
654 selection line, and the order of presentation of the stimuli in the arena were included as random
655 factors in the model. We evaluated the adequacy of our fitted model using scaled-residuals
656 quantile-quantile plots, residual versus predicted values plots and a zero-inflation test in the
657 DHARMa package[79].
658
659 ***Group collective motion during predator inspections.*** We analyzed positional data for each
660 group by binning the observations in a grid, with 20 x 20 mm cells. For each trial, we calculated
661 a density map, where the value for each grid cell was the fraction of all observations that
662 occurred within that cell. The resulting density maps are a normalized representation on how
663 often each grid cell was visited by individuals in our groups of eight fish when exposed to
664 different stimuli (Fig. 2A). We used information from positional data to calculate summary
665 statistics in different areas of interest. Predator model assays presented unique spatial patterns
666 in areas closer to the stimulus presented, with higher densities in the tail area of the predator
667 model (Fig. 2A). Based on these factors, we calculated two new summary variables for each
668 group: i) median polarization of the group when the average position of the group was <200
669 mm to the predator model and novel object assays; and ii) median polarization of the group in
670 locations closer to the head (y-position > 0) and the tail (y-position < 0) in predator model
671 assays. We used LMMs with these new calculated variables as dependent variables in the
672 model to test for potential differences between polarization-selected and control lines.
673 Selection regime, the type of stimulus presented or location in the tank were included as fixed
674 effects, with a random intercept for each replicated selection line and the order of presentation
675 of stimuli as random factors. [74,75]Model diagnostics showed that residual distributions were
676 roughly normal with no evidence of heteroscedasticity. We obtained post-hoc comparisons of
677 the response between selection line regimes at different levels of other fixed effects in the

678 previous models using the emmeans package[76] with the tukey-adjustment method for multiple
679 comparisons.
680
681 **Brain morphology of female guppies following artificial selection**
682 We assessed neuroanatomical features of polarization-selected and control F3 females,
683 approximately six months old (polarization-selected: n = 15, standard length mean [95% CIs]
684 = 238 mm [235, 242]; control: n = 15, standard length mean [95% CIs] = 237 mm [232, 241]).
685 We euthanized animals with an overdose of benzocaine and fixated the whole fish in 2%
686 glutaraldehyde and 4% paraformaldehyde in phosphate buffered saline (PBS) for five days.
687 Following two PBS washes, the brains were dissected out and stained for 48 h in 1%
688 osmiumtetraoxide. We embedded the stained brains in 3% agar and scanned them using
689 microcomputed tomography (microCT, Skyscan 1172, Bruker microCT, Kontich,
690 Belgium). The scanner operated at a voltage of 80 kV, a current of 125 µm, with a 0.5 mm
691 aluminum filter. Images were acquired using an isotropic pixel size of 2.4 µm. We
692 reconstructed cross-sections from scanned images following a in NRecon (Bruker microCT)
693 following a protocol successfully implemented in a previous study evaluating neuroanatomical
694 differences between guppies up- and down-selected for relative brain size[53]. This protocol
695 allowed us to obtain measurements of whole brain size volume and brain region volume in 11
696 major brain regions in the guppy brain: olfactory bulbs, ventral telencephalon, dorsal
697 telencephalon, thalamus, hypothalamus, nucleus glomerulus, torus semicircularis, optic tectum
698 cup, central optic tectum, cerebellum, and medulla oblongata (Fig. 4B). We chose all regions
699 that we could safely identify in the brain scans based on an adult swordtail brain atlas[80] and our
700 own knowledge in fish neuroanatomy. Extended details on guppy brain region reconstruction
701 from digital images can be found in ([53]). Two brains from polarization-selected lines were
702 damaged during the protocol, which reduced the sample size to 28 samples.
703
704 We tested for overall differences in relative brain size between polarization-selected and
705 control lines using a linear mixed model (LMM) with brain volume as dependent variable,
706 body size (standard length) as covariate, selection regime as fixed effect, and replicate as
707 random effect. For each brain region, we used two different approaches to determine whether
708 polarization-selected and control lines differ in relative brain region size. First, we used 11
709 independent LMMs with each region's volume as dependent variable, whole brain volume
710 (excluding the volume of the region of interest) as covariate, selection regime as fixed effect,
711 and replicate as random effect. LMMs were implemented in in R (v4.1.3) and RStudio

712 (v2022.07.0)[71,73] using lme4 and lmerTest packages[74,75]. Second, to take into consideration that
713 brain region volumes may be interdependent, we used a more conservative approach and
714 analyzed the data using a Bayesian multilevel model that included 11 brain regions as
715 dependent variables in a fully multivariate context. The full model included an analogous
716 structure to those used in the independent LMMs for each brain region. Parameter values were
717 estimated using the brms interface[81,82] to the probabilistic programming language Stan[83]. We
718 used default prior distributions with student-t distribution (3, 0, 2.5) for all parameters. The
719 model estimated residual correlations among all brain region volumes with a Lewandowski-
720 Kurowicka-Joe (LKJ) prior with $\eta = 1$, which is uniform over the range −1 to 1. Posterior
721 distributions were obtained using Stan's no-U-turn HMC with six independent Markov chains
722 of 4000 iterations, discarding the first 2000 iterations per chain as warm-up and resulting in
723 12000 posterior samples overall. Convergence of the six chains and sufficient sampling of
724 posterior distributions were confirmed by a scale reduction factor below 1.01, and an effective
725 size of at least 10% of the number of iterations. For each model, posterior samples were
726 summarized on the basis of the Bayesian point estimate (median), SE (median absolute
727 deviation), and posterior uncertainty intervals by HDIs.
728
729 **Visual information processing in response to predation threat**
730
731 *Visual acuity*
732 We evaluated the ability to perceive detail (visual acuity) in 9-12 months old female guppies
733 (polarization-selected: n = 59, standard length [95% CIs] = 270 mm [266, 274], control: n =
734 57, standard length [95% CIs] = 271mm [268, 275]). For this, we assessed their optomotor
735 response, an innate orient behavior induced by whole-field visual stimulation[84], a widely used
736 method to assess visual acuity across tax ([reviewed in 85]). Extended methods and the optimization
737 procedure for the stimuli used here can be found in ([28]). Briefly, we projected a video recording
738 with rotating vertical black and white bands of six different widths (stimuli) on the walls of a
739 white ring-shaped arena of 25/50 cm of inner/outer diameter. Previous optimization of the
740 methods found that the use of these stimuli allowed us to evaluate the optomotor response at
741 the lower end of the species' acuity[28]. We placed individual fish in between the inner wall of
742 the arena and a transparent ring of 40 cm diameter. After a two-minute acclimation period, we
743 recorded their response towards six different rotating stimuli and the static images of these
744 stimuli using a Sony Cam HDR-DR11E recorder. Each stimulus was presented for one minute
745 in random order. We manually scored the videos, recording the time that fish spent circling in

746 the direction of the stimuli (clockwise) at a constant moving pattern using BORIS[77]. Behavioral
747 scoring was performed blind to the treatment since only running numbers identified recordings.
748 Likewise, scoring was blind to the rotation and bandwidth of the stripes since only the fish, but
749 not the rotating stimuli, were visible during scoring. From the scoring, we calculated the
750 proportion of time that a fish spent swimming in the direction of rotation of the stimuli, out of
751 the total time that the different vertical black and white bands were presented to them.
752
753 *Temporal resolution*
754 Two weeks after visual acuity tests were completed in all fish, we measured the ability to track
755 movement stimuli of different speeds (temporal resolution) in the same females from the
756 polarization-selected (n = 58) and control lines (n= 55). We did not keep track of fish identity
757 as fish were kept in groups with conspecifics of the same selection line and replicate between
758 experiments. To evaluate temporal resolution, we placed fish in a white arena (50 cm diameter,
759 4 cm water depth) and exposed them to a projection of black and white bands of 3.5 cm width
760 on the walls rotating clockwise and counterclockwise at four different angular speeds (14.4,
761 25, 36 and 45 degrees/sec). We chose this bandwidth to focus on the assessment of fish
762 response towards direction and speed changes, as this stimulus showed a maximal optomotor
763 response in prior visual acuity tests[28]. The movement of each individual was recorded for a
764 total of 1380 seconds with a Sony Cam HDR-DR11E; a 300 seconds acclimation period and
765 1080 seconds of clockwise and counterclockwise rotation of vertical bands at multiple speeds.
766 Specifically, during each individual test, the 8 stimulus combinations (4 speeds, 2 directions)
767 were presented separately five independent times for 23 sec. The total time of each individual
768 test was 920 sec (23 sec per stimulus x 5 times during the test x 8 stimulus combinations). We
769 randomized the order of presentation of different stimuli a priori, but this order was consistent
770 for all fish. The stimulus changed speed with smooth transitions of 3 sec, accelerating or
771 decelerating to the next speed.
772
773 To quantify speed and direction changes of fish in our experimental setup, we automated
774 behavioral scoring and obtained positional data using the Loopy Deep Learning Module
775 (Loopbio 2020) in MATLAB (v. 2020a). X and y coordinates were transformed into a polar
776 coordinate system centered on 0 and estimated from positional data. We calculated fish
777 orientation by taking the difference in the fish's position between frames and defined their
778 relative orientation (with respect to the arena) with the arcsin ($\sin(\theta - \vartheta)$), where θ was the

779 orientation of the fish and ϑ is the angle of the arena radius going through the fish position.
780 Positive values represent a fish swimming clockwise around the arena, while negative values
781 represent swimming counterclockwise. For each frame, we identified whether the fish was
782 swimming in the same direction of the stimulus projected and calculated the total proportion
783 of time swimming in the direction of the stimulus. We also calculated the speed (in degrees per
784 second) of the fish at each frame by using the dot product of the
785 positional vector between consecutive frames. Using these values, we calculated for each
786 individual the average total speed for each of the stimuli presented, and the average speed
787 deviation between the speed of the stimulus presented and the speed of the fish.
788
789 *Eye size*
790 After the temporal resolution experiments were completed, we measured eye size in the
791 females from polarization-selected lines (n = 57) and control lines (n =55) that were previously
792 assessed for visual acuity and temporal resolution. For morphological measurements, we
793 anesthetized fish with 0.2 mg/l of benzocaine and took pictures of their left side. We measured
794 eye diameter and body length in these pictures using ImageJ[86]. Relative eye size was calculated
795 as the ratio of these two variables. Image analyses were performed by a single scorer who was
796 blind to the selection line treatment in the photographs.
797
798 *Statistics*
799 Analyses were conducted in in R (v4.1.3) and RStudio (v2022.07.0)[71,73]. We analyzed
800 potential differences in optomotor response, temporal resolution and eye size between
801 polarization-selected and control females using LMM's. For the visual acuity trials, the
802 proportion of time rotating was the dependent variable of the model. Fixed effects included
803 selection line regime and bandwidth of the rotating stimuli. To account for differences in
804 activity between fish, we used the proportion of time moving when presented with a static
805 image of the stimuli as a covariate in the model. A random intercept for each replicated
806 selection line, identity of the fish, and an observation-level variable were included as random
807 factors in the model. For temporal resolution, we used selection line regime, the speed of
808 rotation and the direction of rotation as fixed effects. The full model included the interaction
809 between the selection regime with both speed and direction of rotation. This model included
810 the identity of the fish, and a random intercept for each replicated selection line as random
811 factors.
812

For eye size, eye diameter and relative eye size were dependent variables and models included selection regime as a fixed effect and a random intercept for each replicated selection line as a random factor. Model diagnostics showed that residual distributions were roughly normal with no signs of heteroscedasticity in optomotor response and eye size analyses. Model diagnostics on both models for temporal resolution analyses indicated unequal residual variance across the range of predicted values and a potential unequal influence of outliers. While estimates in linear mixed-effects models (LMMs) are argued to be robust to violations of such assumptions[87], we used the robustlmm package to compare the estimates obtained with LMM's to robust models with the same predictors that provide reduced weights to outliers in the data[88]. Results were consistent regarding the modelling approach (Supplementary Table 11). We obtained post-hoc comparisons of the response between selection line regimes at different levels of other fixed effects in the previous models using the emmeans package[76] with the tukey-adjustment method for multiple comparisons.

Acknowledgements

We thank D. Sumpter for important contributions to the conceptualization of the artificial selection procedure. We thank two anonymous reviewers for insightful comments in earlier versions of this manuscript. We thank A. Rennie, E. Trejo, M. Amcoff and A. Boussard for help with fish husbandry. **Funding**: This work was supported by the Knut and Alice Wallenberg Foundation (102 2013.0072 to N.K., and K.P.), the Canada 150 Research Chair Program, and the European Research Council (680951 to J.E.M.), the Swedish Research Council (2016-03435 to N.K., 2017-04957 to A.K., and 2018-04076 to J.H-R.), and the Whitten Lectureship in Marine Biology, University of Cambridge (to J.H-R.). **Author contributions**: N.K., K.P and J.E.M. contributed to conceptualization and funding acquisition of the project. A.K., A.S., M.R., S.D.B., J.H-R., H.Z., K.P., and N.K. contributed to the design of the selection procedure. A.C-L., A.K., A.S., A.F-E., M.R., S.D.B. conducted research to obtain collective behavior data and predator inspection data. A.K. H.Z. and K.P. conducted research to obtain neuroanatomical data. A.C-L., M.G-O., and J.H-R. conducted research to obtain visual capacities data. A. C-L. and W.vdB. performed formal analyses and visualization. A.C-L., J.E.M, and N.K. wrote the original draft. All authors contributed to the final version of the manuscript. **Competing interests**: The authors declare that they have no competing interests. **Data and materials availability**: All data and code needed to evaluate the

conclusions in the paper will be deposited in an online repository. Additional data related to this paper may be requested from the authors.

References

1. Krause, J. & Ruxton, G. D. *Living in Groups*. (Oxford University press, 2002).
2. Pitcher, T. J. Functions of Shoaling Behaviour in Teleosts. in *The Behaviour of Teleost Fishes* (ed. Pitcher T. J.) 294–337 (Springer, Boston, MA, 1986).
3. Strandburg-Peshkin, A. *et al.* Visual sensory networks and effective information transfer in animal groups. *Current biology* **23**, R711 (2013).
4. Pitcher, T. J. Shoaling and Schooling in Fishes Evaluations of compliance with the FAO (UN) Code of Conduct for Responsible Fisheries View project Haida Gwaii ecosystem models View project. (1998).
5. Partridge, B. L. & Pitcher, T. J. The sensory basis of fish schools: Relative roles of lateral line and vision. *Journal of Comparative Physiology □ A* **135**, 315–325 (1980).
6. Blaxter, J. H. S., Gray, J. A. B. & Denton, E. J. Sound and Startle Responses in Herring Shoals. *Journal of the Marine Biological Association of the United Kingdom* **61**, 851–869 (1981).
7. Couzin, I. D., Krause, J., Franks, N. R. & Levin, S. A. Effective leadership and decision-making in animal groups on the move. *Nature* **433**, 513–516 (2005).
8. Parrish, J. K. & Edelstein-Keshet, L. Complexity, Pattern, and Evolutionary Trade-Offs in Animal Aggregation. *Science (1979)* **284**, 99–101 (1999).
9. Herbert-Read, J. E. *et al.* How predation shapes the social interaction rules of shoaling fish. *Proceedings of the Royal Society B: Biological Sciences* **284**, 20171126 (2017).
10. Barton, R. A. Neocortex size and behavioural ecology in primates. *Proceedings of the Royal Society B: Biological Sciences* **263**, 173–177 (1996).
11. Burish, M. J., Kueh, H. Y. & Wang, S. S. H. Brain Architecture and Social Complexity in Modern and Ancient Birds. *Brain Behav Evol* **63**, 107–124 (2004).
12. Triki, Z., Levorato, E., McNeely, W., Marshall, J. & Bshary, R. Population densities predict forebrain size variation in the cleaner fish Labroides dimidiatus. *Proceedings of the Royal Society B* **286**, 20192108 (2019).
13. Chee, S. S. A. *et al.* Social status, breeding state, and GnRH soma size in convict cichlids (Cryptoheros nigrofasciatus). *Behavioural Brain Research* **237**, 318–324 (2013).
14. Shaw, E. Schooling Fishes: The school, a truly egalitarian form of organization in which all members of the group are alike in influence, offers substantial benefits to its participants . *Am Sci* **2**, 166–175 (1978).
15. Pollen, A. A. *et al.* Environmental complexity and social organization sculpt the brain in Lake Tanganyikan cichlid fish. *Brain Behav Evol* **70**, 21–39 (2007).
16. O'Connell, L. A. & Hofmann, H. A. Genes, hormones, and circuits: An integrative approach to study the evolution of social behavior. *Front Neuroendocrinol* **32**, 320–335 (2011).
17. Stednitz, S. J. *et al.* Forebrain Control of Behaviorally Driven Social Orienting in Zebrafish. *Current biology* **28**, 2445-2451.e3 (2018).
18. Gonda, A., Herczeg, G. & Merilä, J. Habitat-dependent and -independent plastic responses to social environment in the nine-spined stickleback (Pungitius pungitius) brain. *Proceedings of the Royal Society B: Biological Sciences* **276**, 2085–2092 (2009).

19. Shinozuka, K. & Watanabe, S. Effects of telencephalic ablation on shoaling behavior in goldfish. *Physiol Behav* **81**, 141–148 (2004).
20. Loomis, C. *et al.* An Adult Brain Atlas Reveals Broad Neuroanatomical Changes in Independently Evolved Populations of Mexican Cavefish. *Front Neuroanat* **13**, 88 (2019).
21. Kotrschal, A. *et al.* Rapid evolution of coordinated and collective movement in response to artificial selection. *Sci Adv* **6**, eaba3148 (2020).
22. Magurran Anne E. *Evolutionary Ecology: The Trinidadian Guppy*. (Oxford University Press, 2005).
23. Bierbach, D. *et al.* Using a robotic fish to investigate individual differences in social responsiveness in the guppy. *R Soc Open Sci* **5**, 181026 (2018).
24. Szorkovszky, A. *et al.* Assortative interactions revealed by sorting of animal groups. *Anim Behav* **142**, 165–179 (2018).
25. Dugatkin, L. A. & Godin, J. G. J. Predator inspection, shoaling and foraging under predation hazard in the Trinidadian guppy, Poecilia reticulata. *Environ Biol Fishes* **34**, 265–276 (1992).
26. Veilleux, C. C. & Kirk, E. C. Visual Acuity in Mammals: Effects of Eye Size and Ecology. *Brain Behav Evol* **83**, 43–53 (2014).
27. Caves, E. M., Sutton, T. T. & Johnsen, S. Visual acuity in ray-finned fishes correlates with eye size and habitat. *Journal of Experimental Biology* **220**, 1586–1596 (2017).
28. Corral-López, A., Garate-Olaizola, M., Buechel, S. D., Kolm, N. & Kotrschal, A. On the role of body size, brain size, and eye size in visual acuity. *Behav Ecol Sociobiol* **71**, 1–10 (2017).
29. Caves, E. M., Brandley, N. C. & Johnsen, S. Visual Acuity and the Evolution of Signals. *Trends in Ecology and Evolution* vol. 33 358–372 Preprint at https://doi.org/10.1016/j.tree.2018.03.001 (2018).
30. Neave, D. A. The development of visual acuity in larval plaice (Pleuronectes platessa L.) and turbot (Scophthalmusmaximus L.). *J Exp Mar Biol Ecol* **78**, 167–175 (1984).
31. Anstis, S., Hutahajan, P. & Cavanagh, P. Optomotor test for wavelength sensitivity in guppyfish (Poecilia reticulata). *Vision Res* **38**, 45–53 (1998).
32. Haug, M. F., Biehlmaier, O., Mueller, K. P. & Neuhauss, S. C. F. Visual acuity in larval zebrafish: Behavior and histology. *Front Zool* **7**, 1–7 (2010).
33. Corral-López, A. *et al.* Female brain size affects the assessment of male attractiveness during mate choice. *Sci Adv* **3**, e1601990 (2017).
34. Cronin, T. W., Johnsen, S., Marshall, N. J. & Warrant, E. J. *Visual Ecology*. *Visual Ecology* (Princeton University Press, 2014).
35. Kotrschal, A. *et al.* Artificial Selection on Relative Brain Size in the Guppy Reveals Costs and Benefits of Evolving a Larger Brain. *Current Biology* **23**, 168–171 (2013).
36. Fong, S. *et al.* Rapid mosaic brain evolution under artificial selection for relative telencephalon size in the guppy (Poecilia reticulata). *Sci Adv* **7**, eabj4314 (2021).
37. Jolles, J. W., Boogert, N. J., Sridhar, V. H., Couzin, I. D. & Manica, A. Consistent Individual Differences Drive Collective Behavior and Group Functioning of Schooling Fish. *Current Biology* **27**, (2017).
38. Kent, M. I. A., Lukeman, R., Lizier, J. T. & Ward, A. J. W. Speed-mediated properties of schooling. *R Soc Open Sci* **6**, (2019).
39. Sumpter, D. J. T., Szorkovszky, A., Kotrschal, A., Kolm, N. & Herbert-Read, J. E. Using activity and sociability to characterize collective motion. *Philosophical Transactions of the Royal Society B: Biological Sciences* **373**, 20170015 (2018).

40. Mishra, S., Tunstrøm, K., Couzin, I. D. & Huepe, C. Collective dynamics of self-propelled particles with variable speed. *Phys Rev E Stat Nonlin Soft Matter Phys* **86**, 011901 (2012).
41. Klamser, P. P. *et al.* Impact of Variable Speed on Collective Movement of Animal Groups. *Front Phys* **9**, 715996 (2021).
42. Pettit, B., Ákos, Z., Vicsek, T. & Biro, D. Speed Determines Leadership and Leadership Determines Learning during Pigeon Flocking. *Current Biology* **25**, 3132–3137 (2015).
43. Jolles, J. W. *et al.* Group-level patterns emerge from individual speed as revealed by an extremely social robotic fish. *Biol Lett* **16**, (2020).
44. Handegard, N. O. *et al.* The dynamics of coordinated group hunting and collective information transfer among schooling prey. *Current Biology* **22**, 1213–1217 (2012).
45. Ioannou, C. C., Guttal, V. & Couzin, I. D. Predatory fish select for coordinated collective motion in virtual prey. *Science (1979)* **337**, 1212–1215 (2012).
46. Kotrschal, A. *et al.* Brain size affects female but not male survival under predation threat. *Ecol Lett* **18**, 646–652 (2015).
47. van der Bijl, W., Thyselius, M., Kotrschal, A. & Kolm, N. Brain size affects the behavioural response to predators in female guppies (Poecilia reticulata). *Proceedings of the Royal Society B: Biological Sciences* **282**, 20151132 (2015).
48. Magurran, A. E., Seghers, B. H., Carvalho, G. R. & Shaw, P. W. Behavioural consequences of an artificial introduction of guppies (Poecilia reticulata) in N. Trinidad: Evidence for the evolution of anti-predator behaviour in the wild. *Proceedings of the Royal Society B: Biological Sciences* **248**, 117–122 (1992).
49. Clément, R. J. G. *et al.* Collective decision making in guppies: A cross-population comparison study in the wild. *Behavioral Ecology* **28**, 919–924 (2017).
50. Northmore, D. P. M. The Optic Tectum . *Encyclopedia of fish physiology: From genome to environment* **1**, 131–142 (2011).
51. Isa, T., Marquez-Legorreta, E., Grillner, S. & Scott, E. K. The tectum/superior colliculus as the vertebrate solution for spatial sensory integration and action. *Current Biology* **31**, R741–R762 (2021).
52. Jones, M. R., Grillner, S. & Robertson, B. Selective projection patterns from subtypes of retinal ganglion cells to tectum and pretectum: Distribution and relation to behavior. *Journal of Comparative Neurology* **517**, 257–275 (2009).
53. Kotrschal, A. *et al.* Evolution of brain region volumes during artificial selection for relative brain size. *Evolution (N Y)* **71**, 2942–2951 (2017).
54. Kowalko, J. E. *et al.* Loss of schooling behavior in cavefish through sight-dependent and sight-independent mechanisms. *Current Biology* **23**, 1874–1883 (2013).
55. Wullimann, M. F. Neural origins of basal diencephalon in teleost fishes: Radial versus tangential migration. *J Morphol* **281**, 1133–1141 (2020).
56. Mueller, T. What is the Thalamus in Zebrafish? *Front Neurosci* **6**, 64 (2012).
57. Goldberg, J. H., Farries, M. A. & Fee, M. S. Basal ganglia output to the thalamus: Still a paradox. *Trends Neurosci* **36**, 695–705 (2013).
58. Bloch, S. *et al.* Non-thalamic origin of zebrafish sensory nuclei implies convergent evolution of visual pathways in amniotes and teleosts. *Elife* **9**, 1–27 (2020).
59. Corral-Lopez, A. *et al.* Functional convergence of genomic and transcriptomic genetic architecture underlying sociability in a live-bearing fish. *bioRxiv* 2023.02.13.528353 (2023) doi:10.1101/2023.02.13.528353.
60. Kutsukake, N. Complexity, dynamics and diversity of sociality in group-living mammals. *Ecological Research* **24**, 521–531 (2009).
61. Bleckmann, H. The Lateral Line System of Fish. *Fish Physiology* **25**, 411–453 (2006).

62. Puzdrowski, R. L. Peripheral distribution and central projections of the lateral-line nerves in goldfish, Carassius auratus. *Brain Behav Evol* **34**, 110–131 (1989).
63. Vega-Trejo, R. *et al.* Artificial selection for schooling behaviour and its effects on associative learning abilities. *Journal of Experimental Biology* **223**, 235093 (2020).
64. Kozloski, J. & Crawford, J. D. Transformations of an auditory temporal code in the medulla of a sound- producing fish. *Journal of Neuroscience* **20**, 2400–2408 (2000).
65. Finger, T. E. Evolution of gustatory reflex systems in the brainstems of fishes. *Integr Zool* **4**, 53–63 (2009).
66. Lecchini, D. *et al.* Variation in brain organization of coral reef fish larvae according to life history traits. *Brain Behav Evol* **83**, 17–30 (2014).
67. Chen, Y. C. *et al.* Expression change in angiopoietin-1 underlies change in relative brain size in fish. *Proceedings of the Royal Society B: Biological Sciences* **282**, 20150872 (2015).
68. Szorkovszky, A. *et al.* An efficient method for sorting and quantifying individual social traits based on group-level behaviour. *Methods Ecol Evol* **8**, 1735–1744 (2017).
69. Pérez-Escudero, A., Vicente-Page, J., Hinz, R. C., Arganda, S. & De Polavieja, G. G. idTracker: tracking individuals in a group by automatic identification of unmarked animals. *Nature Methods 2014 11:7* **11**, 743–748 (2014).
70. Kotrschal, A. *et al.* Brain size does not impact shoaling dynamics in unfamiliar groups of guppies (Poecilia reticulata). *Behavioural Processes* **147**, 13–20 (2018).
71. Posit team. RStudio: Integrated Development Environment for R. Posit Software, PBC, Boston, MA. URL http://www.posit.co/ (2023).
72. Wickham, H. *et al.* Welcome to the Tidyverse. *J Open Source Softw* **4**, 1686 (2019).
73. R Core Team. R: A Language and Environment for Statistical Computing. R Foundation for Statistical Computing, Vienna, Austria. https://www.R-project.org/ (2021).
74. Bates, D., Sarkar, D., Bates, M. D. & Matrix, L. The lme4 Package. *R package version* **2**, 74 (2007).
75. Kuznetsova, A., Brockhoff, P. B. & Christensen, R. H. B. lmerTest Package: Tests in Linear Mixed Effects Models. *J Stat Softw* **82**, 1–26 (2017).
76. Lenth, R. Package 'lsmeans'. *Am Stat* **34**, 216–221 (2018).
77. Friard, O. & Gamba, M. BORIS: a free, versatile open-source event-logging software for video/audio coding and live observations. *Methods Ecol Evol* **7**, 1325–1330 (2016).
78. Brooks, M. E. *et al.* glmmTMB balances speed and flexibility among packages for zero-inflated generalized linear mixed modeling. *R J* **9**, 378–400 (2017).
79. Hartig, F. DHARMa: residual diagnostics for hierarchical (multi-level/mixed) regression models. *R package version 0.3* (2018).
80. Anken, R. H. & Rahmann, H. Brain atlas of the adult swordtail fish, Xiphophorus helleri, and of certain developmental stages. 88 (1994).
81. Bürkner, P. C. Advanced Bayesian multilevel modeling with the R package brms. *R J* **10**, 395–411 (2018).
82. Bürkner, P. C. brms: An R package for Bayesian multilevel models using Stan. *J Stat Softw* **80**, 1–28 (2017).
83. Carpenter, B. *et al.* Stan: A probabilistic programming language. *J Stat Softw* **76**, (2017).
84. Smith, K. U. & Bojar, S. The nature of optokinetic reactions in mammals and their significance in the experimental analysis of the neural mechanisms of visual functions. *Psychol Bull* **35**, 193–219 (1938).

85. Caves, E. M., Troscianko, J. & Kelley, L. A. A customizable, low-cost optomotor apparatus: A powerful tool for behaviourally measuring visual capability. *Methods Ecol Evol* **11**, 1319–1324 (2020).
86. Schneider, C. A., Rasband, W. S. & Eliceiri, K. W. NIH Image to ImageJ: 25 years of image analysis. *Nature Methods 2012 9:7* **9**, 671–675 (2012).
87. Schielzeth, H. *et al.* Robustness of linear mixed-effects models to violations of distributional assumptions. *Methods Ecol Evol* **11**, 1141–1152 (2020).
88. Koller, M. Robustlmm: An R package for Robust estimation of linear Mixed-Effects models. *J Stat Softw* **75**, 1–24 (2016).

1090 **Figures**
1091

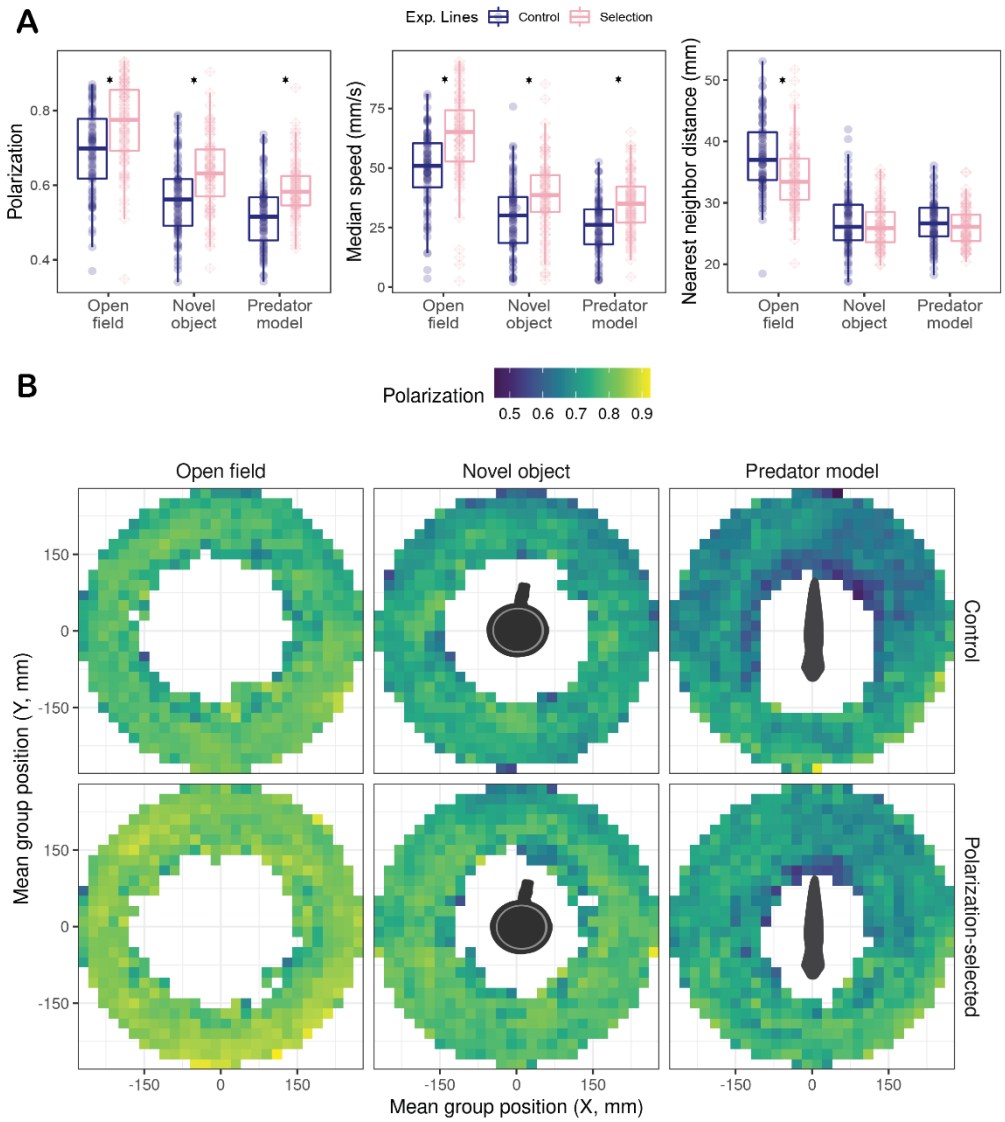

1092
1093
1094 **Fig 1. Collective motion patterns in female guppies artificially selected for higher**
1095 **polarization. A)** Boxplots of median polarization, speed and nearest neighbor distance for
1096 groups of eight individuals of polarization-selected (pink) and control (blue) female guppies
1097 assayed in an open field test (OFT), with a novel object and with a predator model. Horizontal
1098 lines indicate medians, boxes indicate the interquartile range, and whiskers indicate all points
1099 within 1.5 times the interquartile range. Asterisks indicate $p < 0.05$ (see methods;
1100 Supplementary Tables 1-2). **B)** Heatmaps of group polarization across different locations of
1101 the experimental arena when control (top) and polarization-selected (bottom) groups were
1102 exposed to open field, novel object and predator model assays. Grid cells with data for less
1103 than 8 groups were not depicted.
1104
1105
1106
1107
1108
1109

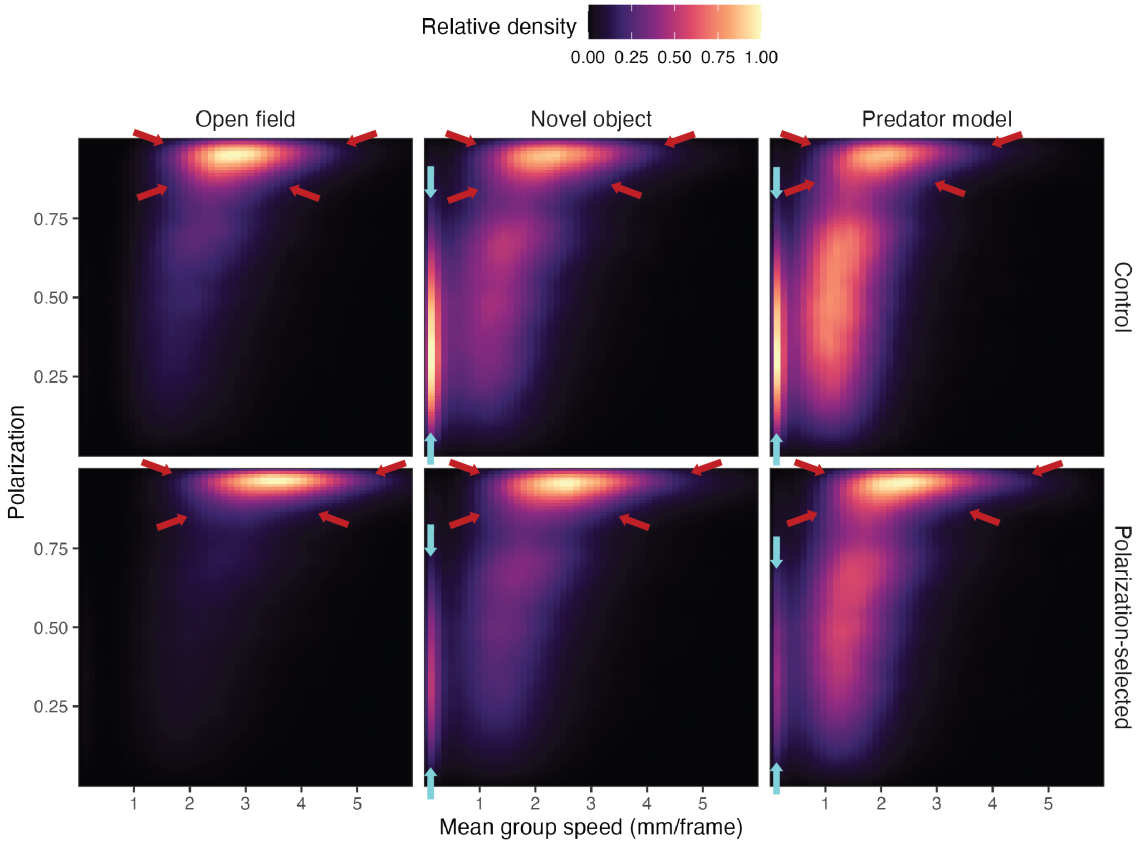

Fig 2. Correlation between group polarization and speed. Heatmaps showing the association between group polarization and speed in control (top) and polarization-selected (bottom) groups of eight guppy females exposed to open field, novel object and predator model assays. Group speed depicts the mean median swimming speed of the individuals in a group in mm per frame. Heatmaps indicate that the overall decrease in polarization in the presence of a novel object and a predator model was associated with a reduction in speed (higher relative density of group speed < 2 mm/frame). The consistent differences in polarization across treatments between polarization-selected and control groups seem to be driven by: i) lower reduction in mean group speed in polarization-selected groups, including periods of no movement (area delimited by blue arrows): and ii) consistent differences in motion characteristics regardless of the presence of stimuli in the assay (lower range of group polarization at group speed >2 mm/frame, area delimited by red arrows).

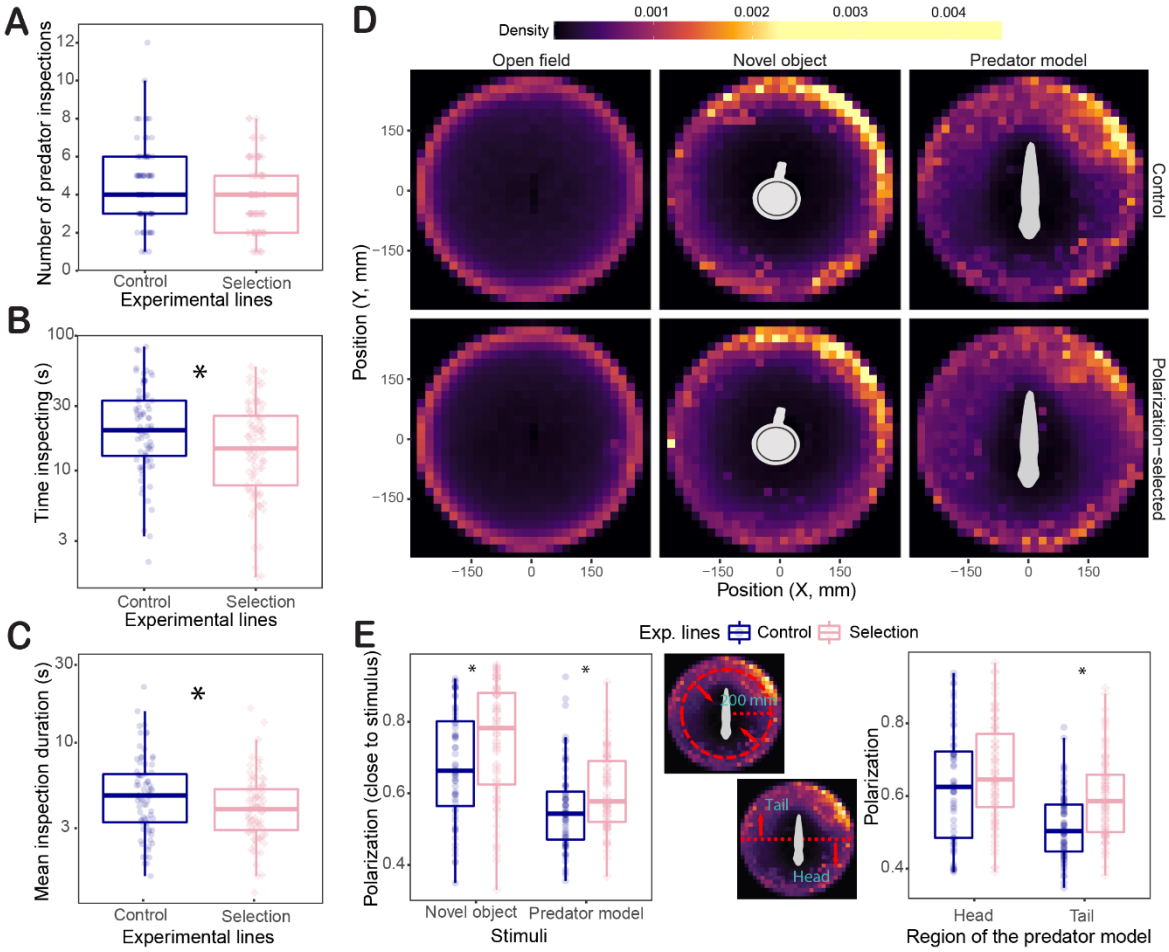

Fig 3. Predator inspection behavior and collective motion. Boxplots of number of predator inspections **(A)**, total time inspecting **(B),** and mean inspection duration **(C)** for individuals when swimming in a group of eight polarization-selected (pink) and control (blue) female guppies in the presence of a predator model. Horizontal lines indicate medians, boxes indicate the interquartile range, and whiskers indicate all points within 1.5 times the interquartile range. Asterisks indicate $p < 0.05$ (see methods, Supplementary Tables 3-5). **(D)** Density maps based on positional data of control (top) and polarization-selected (bottom) groups exposed to open field, novel object and predator model assays. **(E)** Boxplots of median group polarization in locations closer than 200 mm of the stimulus presented (left) and in the head and tail area of a predator model (right) in control (blue) and polarization-selected (pink) guppy groups.

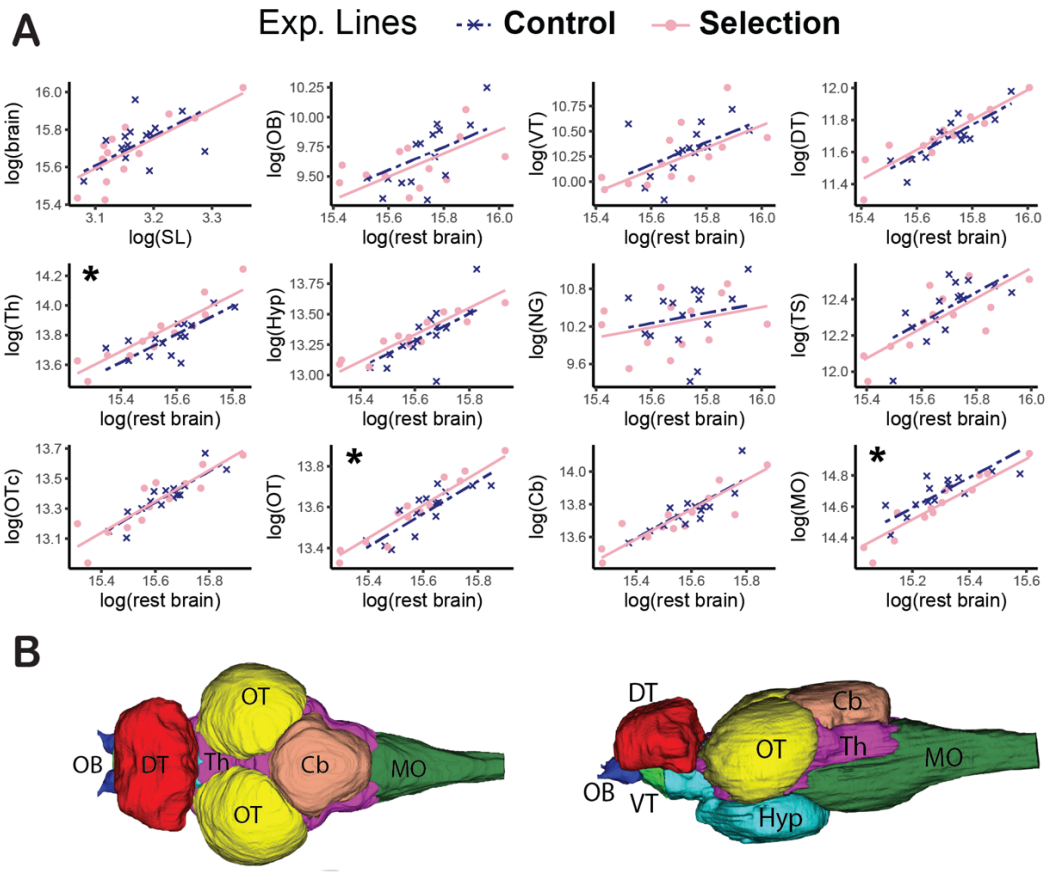

Fig 4. The effect of artificial selection for higher polarization in neuroanatomical allometric relationships. (A) The top left panel shows the allometric relationship between whole brain size volume and standard length of the fish (SL). Remaining panels show the relationship between each separate brain region with the rest of the brain ordered rostrally to caudally. Asterisks indicate brain regions with non-overlapping confidence intervals between polarization-selected females (pink; n = 13) and control females (blue; n = 15) in two consistent statistical analyses (Supplementary Tables 6-7). **(B)** Reconstructed brain regions from microCT - scanned guppy brains. A dorsal (left) and lateral (right) view of a guppy brain with the major brain regions color coded: olfactory bulbs (OB; dark blue), dorsal telencephalon (DT; red), ventral telencephalon (VT; light green), optic tectum (OT; yellow), hypothalamus (Hyp; turquoise), thalamus (Th; purple), cerebellum (Cb; brown), medulla oblongata (MO; dark green). Not visible but measured brain regions include: torus semicircularis, nucleus glomerulus and optic tectum core.

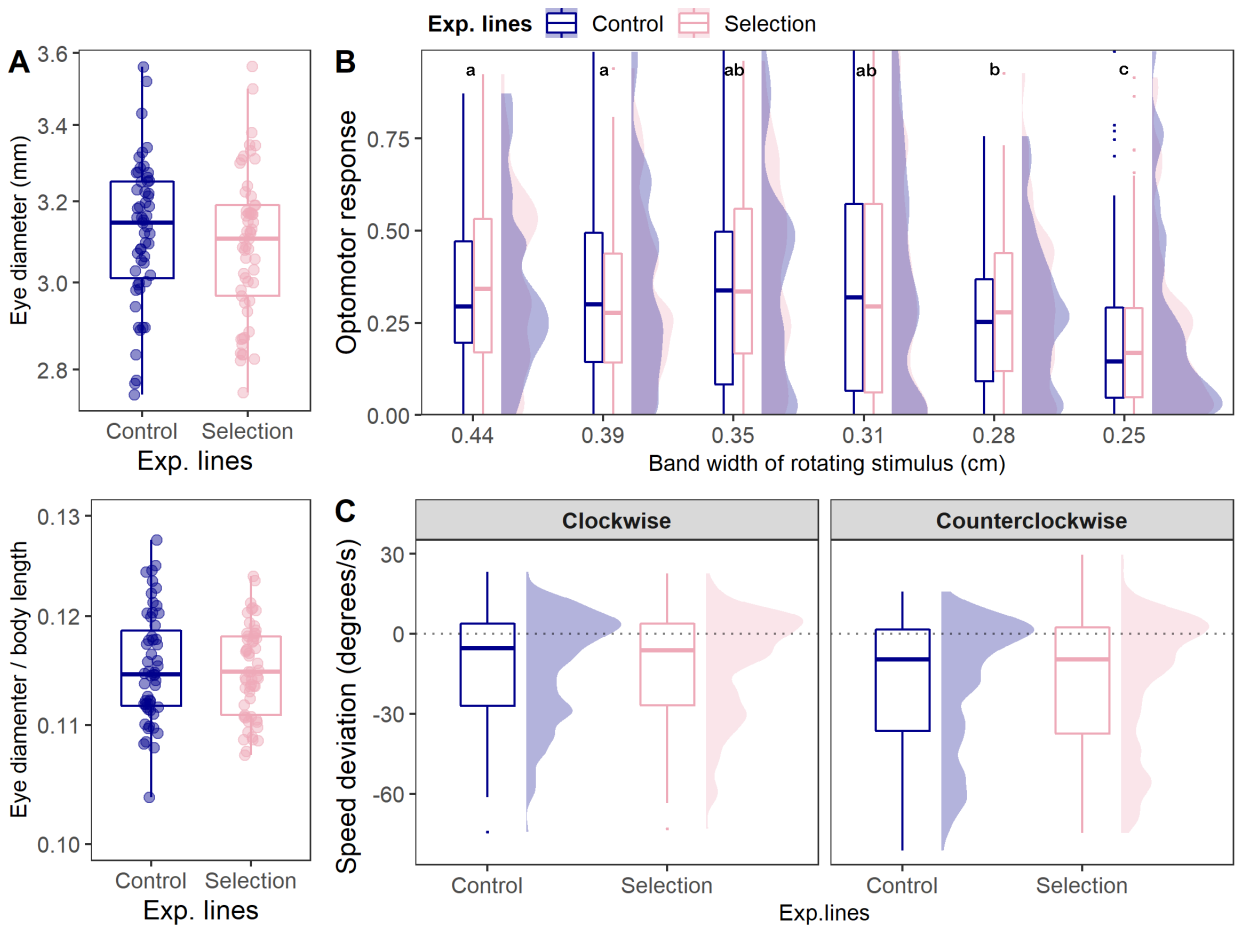

Fig 5. Eye size and visual capacities of female guppies artificially selected for higher polarization. **(A)** Boxplots of eye morphological measurements. **(B)** Boxplots and density plots of the proportion of time following 6 different rotating stimuli with rotating and static gratings of different widths at the lower end of guppy visual acuity (thinner widths represent a higher degree of difficulty to be perceived). **(C)** Boxplots and density plots of the deviation of fish swimming speed in relation to the speed that a rotating stimulus presented. in polarization-selected. For all morphological measurements and vision assays we measured the same polarization-selected (pink; n = 57-59) and control females (blue; n = 55-57). In all boxplots, horizontal lines indicate medians, boxes indicate the interquartile range, and whiskers indicate all points within 1.5 times the interquartile range. Optomotor response average values not sharing any letter are significantly different ($p < 0.05$) in post-hoc contrasts (see Supplementary Table 9b). No significant differences were observed for any comparison between control and polarization-selected fish (see Supplementary Tables 8-10).

Supplementary Figures for:

Changes driven by the evolution of higher group polarization in the guppy are consistent across different predation pressures and associated with neuroanatomical changes

Alberto Corral-Lopez*, Alexander Kotrschal, Alexander Szorkovszky, Maddi Garate-Olaizola, James Herbert-Read, Wouter van der Bijl, Maksym Romenskyy, Hong-Li Zeng, Severine Denise Buechel, Ada Fontrodona-Eslava, Kristian Pelckmans, Judith E. Mank, Niclas Kolm

*corresponding author: alberto.corral@ebc.uu.se

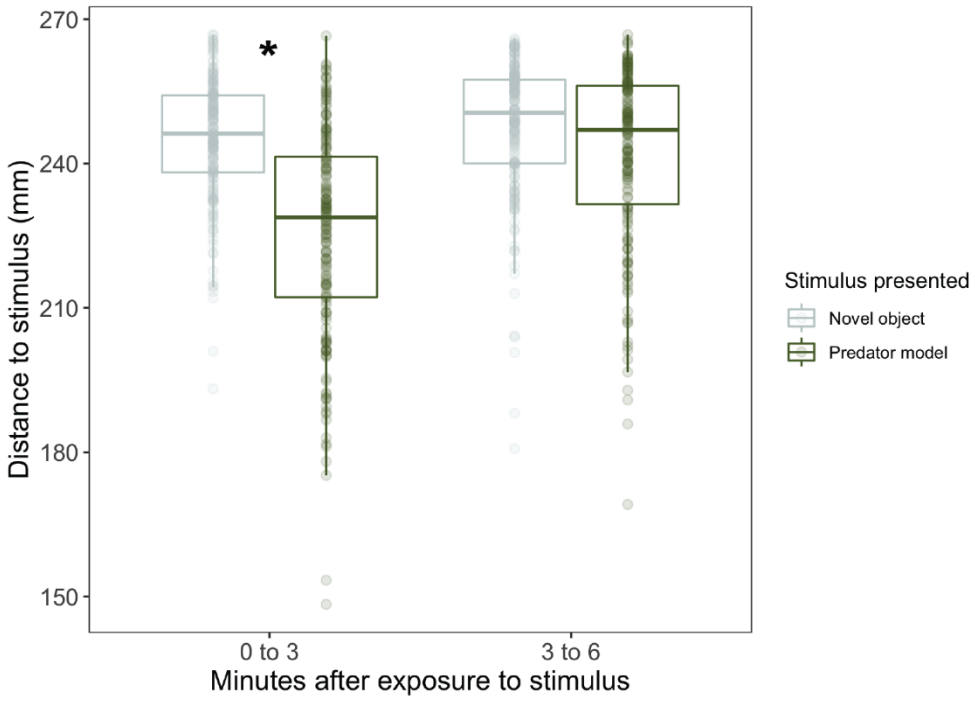

Fig S1. Proximity to stimuli in female guppies artificially selected for higher polarization. Boxplots of median distance to the stimulus combining data for groups of polarization-selected and control female guppies (n = 164) in predator model and novel object assays. Horizontal lines indicate medians, boxes indicate the interquartile range, and whiskers indicate all points within 1.5 times the interquartile range. Asterisks indicate $p < 0.05$.

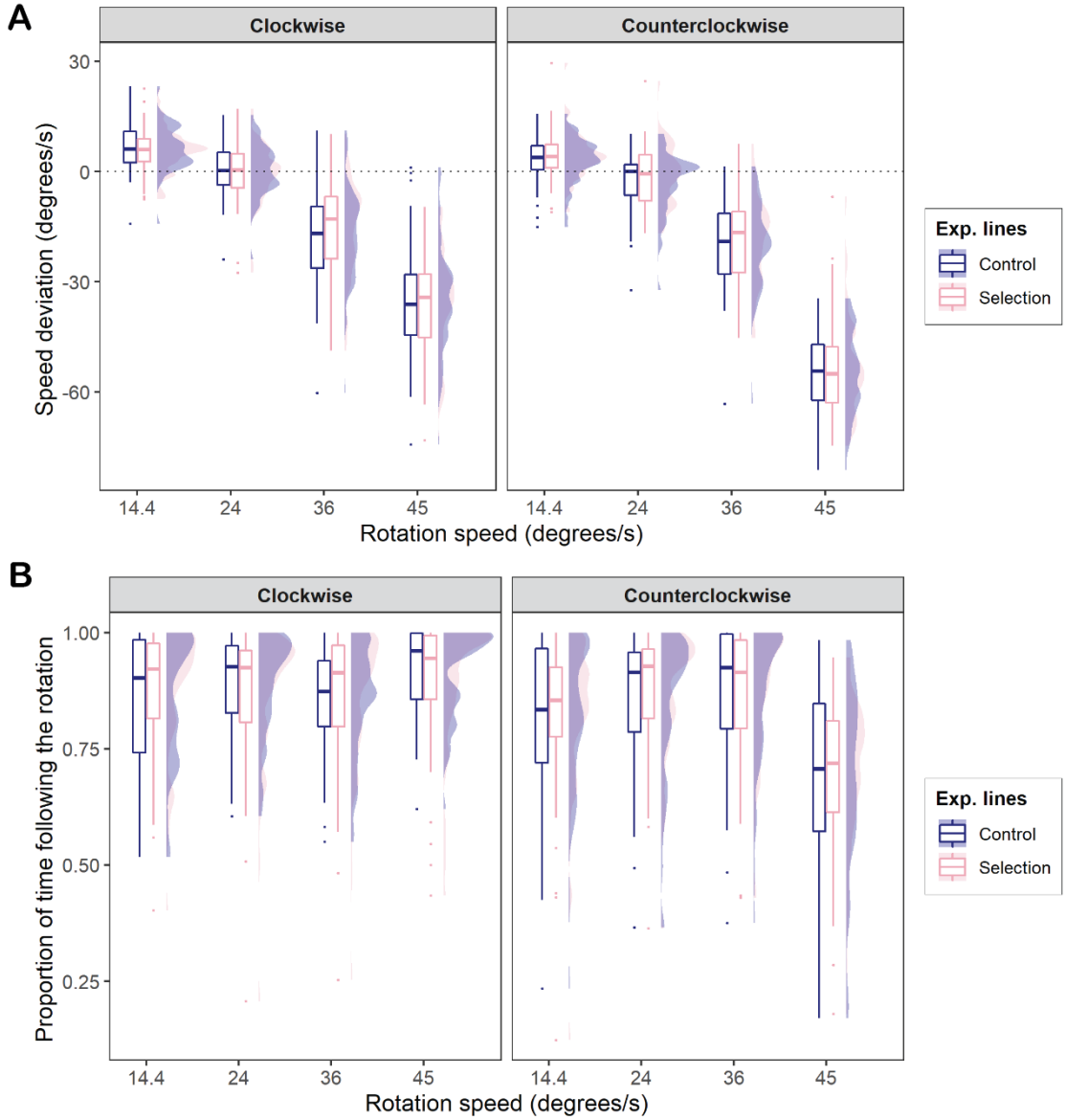

Fig S2. Temporal resolution of female guppies artificially selected for higher polarization. Boxplots and density plots of the deviation of fish swimming speed **(A),** and the proportion of time that fish followed the direction of the stimulus **(B)** in relation to four different rotating stimuli presented at different speeds that rotated clockwise and anti-clockwise to polarization-selected (pink; n = 58) and control females (blue; n = 56). In the boxplots, horizontal lines indicate medians, boxes indicate the interquartile range, and whiskers indicate all points within 1.5 times the interquartile range. No significant differences were observed for any comparison between control and polarization-selected fish (see Tables S9-S10).

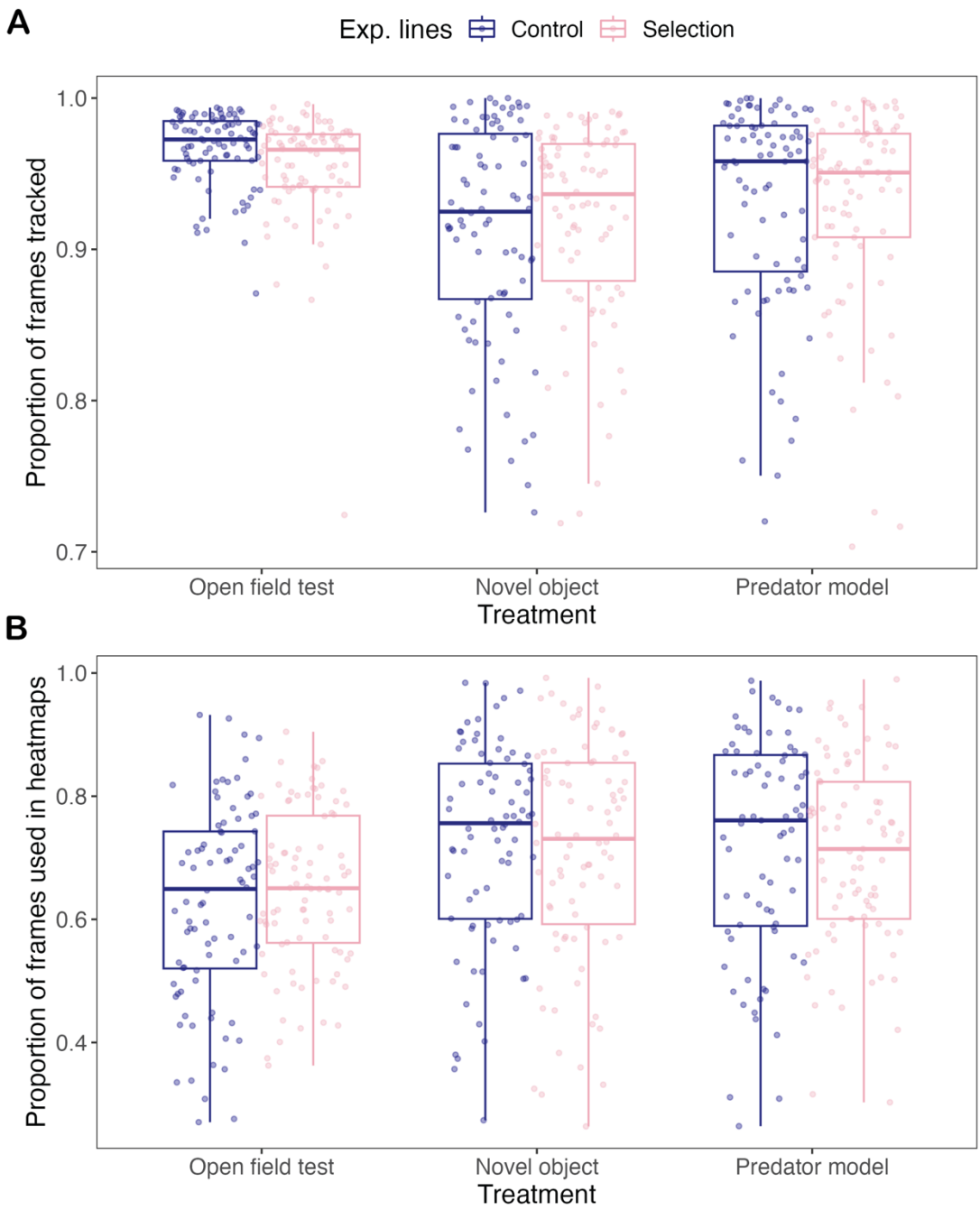

Fig S3. Tracking data reliability between groups. We found no differences between polarization-selected groups (pink) and control groups (blue) in **(A)** the total proportion of frames tracked by idTracker in open field, novel object and predator model assays, or in **(B)** the data used to generate heatmaps that only considered frames in which at least six individuals formed a connected group, with an interindividual distance of 10cm counting as a connection.

Supplementary Tables for:

Changes driven by the evolution of higher group polarization in the guppy are consistent across different predation pressures and associated with neuroanatomical changes

Alberto Corral-Lopez*, Alexander Kotrschal, Alexander Szorkovszky, Maddi Garate-Olaizola, James Herbert-Read, Wouter van der Bijl, Maksym Romenskyy, Hong-Li Zeng, Severine Denise Buechel, Ada Fontrodona-Eslava, Kristiaan Pelckmans, Judith E. Mank, Niclas Kolm

*corresponding author: alberto.corral@ebc.su.se

Table S1. Statistical tests for overall comparisons in tests evaluating polarization-selected and control female guppies in their shoaling patterns when exposed to an open field test (OFT), a novel object (cup) and a predator model.

Polarization

Predictors	*Estimates*	*CI*	*t*	*p*	*df*
(Intercept)	0.80	0.68 – 0.91	14.54	**< 0.001**	17.59
Selection [P]	0.08	0.02 – 0.13	3.90	**0.017**	3.98
treatment [Cup]	-0.12	-0.15 – -0.10	-9.16	**< 0.001**	338.42
treatment [Predator]	-0.17	-0.20 – -0.14	-12.61	**< 0.001**	340.73
Body size	-0.00	-0.00 – -0.00	-2.35	**0.021**	88.01
Selection [P] * treatment [Cup]	-0.01	-0.05 – 0.03	-0.46	0.644	340.46
Selection [S] * treatment [Predator]	-0.00	-0.04 – 0.03	-0.18	0.860	341.08

Median speed

Predictors	*Estimates*	*CI*	*t*	*p*	*df*
(Intercept)	63.25	46.15 – 80.34	7.50	**< 0.001**	35.87
Selection [P]	13.63	8.09 – 19.16	5.96	**< 0.001**	6.29
treatment [Cup]	-20.14	-23.91 – -16.37	-10.51	**< 0.001**	337.87

treatment [Predator]	-24.34	-28.14 – -20.54	-12.60	**< 0.001**	339.82
Body size	-0.06	-0.12 – 0.01	-1.77	0.080	85.64
Selection [P] * treatment [Cup]	-4.55	-9.85 – 0.76	-1.69	0.093	339.52
Selection [S] * treatment [Predator]	-3.95	-9.27 – 1.36	-1.46	0.144	340.05

Nearest neighbor distance

Predictors	*Estimates*	*CI*	*t*	*p*	*df*
(Intercept)	39.17	33.89 – 44.45	14.96	**< 0.001**	43.22
Selection [P]	-3.43	-5.34 – -1.53	-4.55	**< 0.001**	5.31
treatment [Cup]	-10.77	-11.94 – -9.60	-18.13	**< 0.001**	337.80
treatment [Predator]	-10.88	-12.06 – -9.70	-18.17	**< 0.001**	339.69
Body size	-0.01	-0.03 – 0.01	-0.63	0.530	105.88
Selection [P] * treatment [Cup]	2.88	1.24 – 4.53	3.45	**< 0.001**	339.38
Selection [S] * treatment [Predator]	2.82	1.17 – 4.47	3.37	**< 0.001**	339.88

Table S2. Independent contrasts for comparisons between polarization-selected and control female guppies in their shoaling patterns when exposed to an open field test (OFT), a novel object (cup) and a predator model

Polarization

contrast	*treatment*	*estimate*	*SE*	*df*	*lower.CL*	*upper.CL*	*t.ratio*	*p.value*
C - P	OFT	-0.077	0.020	3.980	-0.133	-0.022	-3.898	**0.018**
C - P	Cup	-0.069	0.020	4.078	-0.124	-0.014	-3.435	**0.026**
C - P	Predator	-0.074	0.020	4.106	-0.129	-0.019	-3.698	**0.020**

Median speed

contrast	*treatment*	*estimate*	*SE*	*df*	*lower.CL*	*upper.CL*	*t.ratio*	*p.value*
C - P	OFT	-13.627	2.288	6.292	-19.164	-8.091	-5.956	**0.001**
C - P	Cup	-9.079	2.311	6.560	-14.619	-3.538	-3.928	**0.006**
C - P	Predator	-9.673	2.321	6.618	-15.226	-4.121	-4.168	**0.005**

Nearest neighbor distance

contrast	*treatment*	*estimate*	*SE*	*df*	*lower.CL*	*upper.CL*	*t.ratio*	*p.value*
C - P	OFT	3.434	0.754	5.309	1.530	5.339	4.555	**0.005**
C - P	Cup	0.552	0.761	5.510	-1.350	2.455	0.726	0.498
C - P	Predator	0.613	0.764	5.560	-1.292	2.517	0.802	0.455

Table S3. Statistical tests for comparisons in tests evaluating polarization-selected and control female guppies in their anti-predator behavior when exposed to a predator model

Number of inspections

Predictors	*Incidence Rate Ratios*	*CI*	*t*	*p*
(Intercept)	4.47	3.64 – 5.50	14.19	**< 0.001**
Selection [P]	0.87	0.75 – 1.01	-1.85	0.0645

Total time inspecting

Predictors	*Incidence Rate Ratios*	*CI*	*t*	*p*
(Intercept)	24.04	18.02 – 32.07	21.64	**< 0.001**
Selection [P]	0.79	0.66 – 0.95	-2.52	**0.011**

Mean inspection duration

Predictors	*Incidence Rate Ratios*	*CI*	*t*	*p*
(Intercept)	5.62	4.84 – 6.53	22.63	**< 0.001**
Selection [P]	0.82	0.69 – 0.96	-2.49	**0.013**

Table S4a. Statistical tests for overall comparisons of group polarization in polarization-selected and control female guppies when the average position of the group was shorter than 200 mm to the stimulus presented in the arena in tests that exposed these fish to a predator model and a novel object (cup).

Polarization (closer than 200 mm from the predator model)					
Predictors	*Estimates*	*CI*	*t*	*p*	*df*
(Intercept)	0.68	0.60 – 0.75	25.78	**< 0.001**	3.87
Selection [P]	0.07	0.02 – 0.12	2.96	**0.003**	273.80
treatment [Predator model]	-0.12	-0.16 – -0.08	-5.34	**< 0.001**	146.76
Replicate [Rep2]	0.00	-0.04 – 0.04	0.05	0.958	143.72
replicate [Rep3]	0.01	-0.03 – 0.05	0.32	0.749	142.38
Selection [P] * treatment [Predator model]	-0.03	-0.08 – 0.03	-0.83	0.405	143.99

Table S4b. Statistical tests for independent contrasts of group polarization in polarization-selected and control female guppies when swimming at a distance closer than 200 mm to the stimulus presented in the arena in tests that exposed these fish to a predator model and a novel object (cup).

contrast	*treatment*	*estimate*	*SE*	*df*	*lower.CL*	*upper.CL*	*t.ratio*	*p.value*
C - P	Cup	-0.070	0.024	273.79	-0.116	-0.023	-2.956	**0.003**
C - P	Predator	-0.044	0.022	272.27	-0.088	-0.000	-1.984	**0.048**

Table S5a. Statistical tests for overall comparisons of group polarization in polarization-selected and control female guppies when the average position of the group was located closer to the tail area or closer to the head area of the predator model

Polarization					
Predictors	*Estimates*	*CI*	*Statistic*	*p*	*df*
(Intercept)	0.62	0.54 – 0.71	22.54	**< 0.001**	3.15
Selection [P]	0.04	-0.03 – 0.10	1.53	0.191	4.58
location [tail]	-0.11	-0.14 – -0.07	-5.47	**< 0.001**	156.96
line [Social] * location [tail]	0.04	-0.01 – 0.09	1.64	0.103	150.99

Table S5b. Statistical tests for independent contrasts of group polarization in polarization-selected and control female guppies when the average position of the group was located closer to the tail area or closer to the head area of the predator model

contrast	*location*	*estimate*	*SE*	*df*	*lower.CL*	*upper.CL*	*t.ratio*	*p.value*
C - P	Head	-0.037	0.024	4.58	-0.102	0.027	-1.534	0.191
C - P	Tail	-0.080	0.023	3.63	-0.146	-0.013	-3.483	**0.030**

Table S6. Results from independent Linear Mixed Models evaluating differences in relative brain and relative brain region size between polarization-selected and control female guppies.

Region	Coefficent	Estimate	SE	df	t	P-value
Whole brain	Intercept	10.706	0.929	22.992	11.520	**< 0.001**
	Sel. Line (Polarization)	-0.015	0.037	23.296	-0.415	0.682
	Log (SL)	1.581	0.292	22.899	5.401	**< 0.001**
Olfactory bulbs	Intercept	-5.639	4.048	24.311	-1.393	0.176
	Sel. Line (Polarization)	-0.054	0.071	23.443	-0.759	0.455
	Log (rest of brain)	0.973	0.257	24.319	3.782	**< 0.001**
Ventral telencephalon	Intercept	-7.112	4.022	23.970	-1.768	0.0897
	Sel. Line (Polarization)	-0.054	0.070	23.366	-0.762	0.453
	Log (rest of brain)	1.107	0.255	23.968	4.329	**< 0.001**
Dorsal telencephalon	Intercept	-3.002	1.502	25.000	-1.998	0.0567
	Sel. Line (Polarization)	0.029	0.027	25.000	1.096	0.2837
	Log (rest of brain)	0.935	0.095	25.000	9.780	**< 0.001**
Thalamus	Intercept	-1.019	1.805	25.000	-0.565	0.577
	Sel. Line (Polarization)	0.073	0.033	25.000	2.187	**0.038**
	Log (rest of brain)	0.950	0.115	25.000	8.197	**< 0.001**
Hypothalamus	Intercept	-3.858	2.745	25.000	-1.405	0.172
	Sel. Line (Polarization)	0.048	0.049	25.000	0.974	0.339
	Log (rest of brain)	1.098	0.175	25.000	6.259	**< 0.001**
Nucleus glomerulus	Intercept	-2.352	9.716	25.000	-0.242	0.811
	Sel. Line (Polarization)	-0.067	0.176	25.000	-0.381	0.706
	Log (rest of brain)	0.807	0.617	25.000	1.308	0.203
Torus semicircularis	Intercept	-0.665	2.368	24.977	-0.281	0.781
	Sel. Line (Polarization)	-0.0325	0.042	24.106	-0.758	0.456
	Log (rest of brain)	0.829	0.150	24.982	5.496	**< 0.001**
Optic tectum cup	Intercept	1.073	0.966	23.494	1.111	0.2780
	Sel. Line (Polarization)	0.042	0.017	23.095	2.409	**0.024**
	Log (rest of brain)	0.800	0.061	23.474	12.933	**< 0.**001
Optic tectum core	Intercept	-2.883	1.658	25.000	-1.739	0.0944
	Sel. Line (Polarization)	0.006	0.030	25.000	0.211	0.8347
	Log (rest of brain)	1.040	0.106	25.000	9.805	**< 0.001**
Cerebellum	Intercept	-0.403	1.458	24.350	-0.277	0.784
	Sel. Line (Polarization)	-0.007	0.026	23.221	-0.275	0.786
	Log (rest of brain)	0.908	0.093	24.358	9.703	**< 0.001**
Medulla oblongata	Intercept	-0.145	1.519	24.920	-0.096	0.9246
	Sel. Line (Polarization)	-0.074	0.028	23.916	-2.656	**0.013**
	Log (rest of brain)	0.969	0.099	24.935	9.761	**< 0.001**

Table S7a Results from a Bayesian multilevel model evaluating differences in relative brain region size between polarization-selected and control female guppies. Stars indicate estimates that do not include zero in the confidence interval range based on the posterior samples drawn from the model.

Covariate	***Estimate***	***Est.Error***	***l.95..CI***	***u.95..CI***	
Medulla_Intercept	0.19	0.32	-0.37	0.77	
Cerebellum_Intercept	0.05	0.50	-1.08	1.04	
Nucleus glomerulus_Intercept	0.09	0.48	-0.84	1.04	
Torus semicircularis_Intercept	0.14	0.44	-0.69	1.03	
Thalamus_Intercept	-0.25	0.34	-0.97	0.31	
Optic tectum cups_Intercept	-0.19	0.51	-1.26	0.89	
Hypothalamus_Intercept	-0.06	0.39	-0.84	0.73	
Olfactory bulbs_Intercept	0.13	0.54	-0.94	1.26	
Ventral telencephalon_Intercept	0.05	0.63	-1.23	1.43	
Dorsal telencephalon_Intercept	-0.09	0.32	-0.72	0.56	
Optic tectum core_Intercept	-0.02	0.28	-0.56	0.54	
Medulla oblongata_Selection	-0.42	0.18	**-0.79**	**-0.06**	*
Medulla oblongata_Rest of the brain	0.91	0.09	**0.74**	**1.09**	*
Cerebellum_Selection	-0.07	0.21	-0.48	0.35	
Cerebellum_Rest of the brain	0.96	0.11	**0.75**	**1.18**	*
Nucleus glomerolus_Selection	-0.21	0.40	-0.98	0.58	
Nucleus glomerulus_Rest of the brain	0.34	0.20	-0.06	0.75	
Torus semicircularis_Selection	-0.24	0.32	-0.87	0.38	
Torus semicircularis_Rest of the brain	0.72	0.16	**0.40**	**1.04**	*
Thalamus_Selection	0.49	0.23	**0.04**	**0.94**	*
Thalamus_Rest of the brain	0.92	0.11	**0.70**	**1.16**	*
Optic tectum cups_Selection	0.32	0.16	**0.00**	**0.63**	*
Optic tectum cups_Rest of the brain	0.88	0.08	**0.72**	**1.06**	*
Hypothalamus_Selection	0.12	0.26	-0.39	0.64	

Hypothalamus_Rest of the brain	0.87	0.13	**0.61**	**1.14**	*
Olfactory bulbs _Selection	-0.27	0.33	-0.93	0.38	
Olfactory bulbs_Rest of the brain	0.62	0.17	**0.29**	**0.95**	*
Ventral telencephalon_Selection	-0.17	0.31	-0.76	0.43	
Ventral telencephalon_Rest of the brain	0.58	0.16	**0.27**	**0.89**	*
Dorsal telencephalon_Selection	0.18	0.21	-0.25	0.60	
Dorsal telencephalon_Rest of the brain	0.91	0.11	**0.69**	**1.13**	*
Optic tectum core_Selection	0.05	0.20	-0.34	0.44	
Optic tectum core_Rest of the brain	0.93	0.10	**0.73**	**1.13**	*

Table S7b. Residual correlations of thalamus, optic tectum cups and medulla oblongata relative volume to other brain regions estimated from a Bayesian multilevel model evaluating differences in relative brain region size between polarization-selected and control female guppies. Stars indicate estimates that do not include zero in the confidence interval range based on the posterior samples drawn from the model.

Medulla oblongata

Brain region	*Estimate*	*Est.Error*	*l.95..CI*	*u.95..CI*	
Cerebellum	-0.32	0.15	**-0.59**	**-0.02**	*
Nucleus glomerulus	-0.26	0.15	-0.53	0.05	
Torus semicircularis	0.07	0.16	-0.25	0.37	
Thalamus	-0.40	0.14	**-0.65**	**-0.12**	*
Optic tectum cups	-0.04	0.17	-0.36	0.29	
Hypothalamus	-0.50	0.12	**-0.72**	**-0.23**	*
Olfactory bulbs	-0.24	0.16	-0.52	0.09	
Ventral telencephalon	-0.15	0.16	-0.44	0.17	
Dorsal telencephalon	-0.12	0.17	-0.43	0.21	
Optic tectum core	-0.22	0.15	-0.51	0.09	

Optic tectum cups

Brain region	*Estimate*	*Est.Error*	*l.95..CI*	*u.95..CI*
Medulla oblongata	-0.04	0.16	-0.36	0.28
Cerebellum	-0.07	0.17	-0.41	0.26
Nucleus glomerulus	-0.07	0.17	-0.40	0.26
Torus semicircularis	0.05	0.17	-0.29	0.38
Thalamus	-0.18	0.16	-0.49	0.15
Hypothalamus	-0.15	0.16	-0.46	0.17

Olfactory bulbs	-0.11	0.17	-0.45	0.23
Ventral telencephalon	0.02	0.17	-0.32	0.36
Dorsal telencephalon	-0.01	0.17	-0.36	0.33
Optic tectum core	-0.06	0.17	-0.39	0.27

Thalamus

Brain region	***Estimate***	***Est.Error***	***l.95..CI***	***u.95..CI***	
Medulla oblongata	-0.40	0.14	**-0.65**	**-0.12**	*
Cerebellum	-0.27	0.16	-0.55	0.05	
Nucleus glomerulus	0.05	0.16	-0.26	0.36	
Torus semicircularis	-0.27	0.16	-0.56	0.06	
Optic tectum cups	-0.18	0.17	-0.49	0.15	
Hypothalamus	-0.15	0.16	-0.44	0.18	
Olfactory bulbs	-0.09	0.16	-0.41	0.24	
Ventral telencephalon	0.27	0.16	-0.05	0.56	
Dorsal telencephalon	-0.05	0.17	-0.37	0.28	
Optic tectum core	0.10	0.16	-0.22	0.41	

Table S8. Statistical tests for comparisons in eye morphology between polarization-selected and control female guppies.

Eye diameter					
Predictors	*Estimates*	*CI*	*Statistic*	*p*	*df*
(Intercept)	3.12	2.95 – 3.29	78.98	**< 0.001**	2.00
Selection [P]	-0.03	-0.24 – 0.19	-0.52	0.658	2.00
Eye diameter / body length					
Predictors	*Estimates*	*CI*	*Statistic*	*p*	*df*
(Intercept)	0.12	0.11 – 0.12	69.97	**< 0.001**	2.00
Selection [P]	-0.00	-0.01 – 0.01	-0.13	0.906	2.00

Table S9a. Statistical tests for comparisons in visual acuity between polarization-selected and control female guppies.

Optomotor response					
Predictors	*Estimates*	*CI*	*Statistic*	*p*	*df*
(Intercept)	0.10	0.03 – 0.17	3.16	**0.008**	12.06
Selection [P]	0.00	-0.08 – 0.09	0.11	0.913	12.88
Band width stimulus [0.28]	0.07	0.00 – 0.14	2.09	**0.036**	570.82
Band width stimulus [0.31]	0.15	0.08 – 0.21	4.20	**< 0.001**	569.22
Band width stimulus [0.35]	0.12	0.05 – 0.19	3.51	**< 0.001**	569.28
Band width stimulus [0.39]	0.18	0.12 – 0.25	5.26	**< 0.001**	574.04
Band width stimulus [0.44]	0.17	0.10 – 0.23	4.75	**< 0.001**	572.07
Optomotor response in static	0.56	0.49 – 0.63	14.92	**< 0.001**	531.69
Selection [P]* Band width stimulus [0.28]	0.01	-0.08 – 0.11	0.26	0.793	569.30
Selection [P]* Band width stimulus [0.31]	0.01	-0.09 – 0.10	0.11	0.915	569.21
Selection [P]* Band width stimulus [0.35]	0.03	-0.06 – 0.13	0.63	0.526	569.18
Selection [P]* Band width stimulus [0.39]	-0.03	-0.13 – 0.06	-0.64	0.520	569.16
Selection [P]* Band width stimulus [0.44]	0.01	-0.09 – 0.10	0.17	0.863	569.22

Table S9b. Independent contrasts for optomotor response observed in fish at rotating stimulus of several band widths

contrast	*estimate*	*SE*	*df*	*lower.CL*	*upper.CL*	*t.ratio*	*p.value*
bw25 - bw28	-0.079	0.024	571.167	-0.149	-0.009	-3.236	**0.016**

bw25 - bw31	-0.148	0.024	569.618	-0.218	-0.079	-6.094	**< 0.001**
bw25 - bw35	-0.137	0.024	569.230	-0.207	-0.068	-5.637	**< 0.001**
bw25 - bw39	-0.168	0.025	577.744	-0.238	-0.097	-6.818	**< 0.001**
bw25 - bw44	-0.169	0.024	573.616	-0.239	-0.099	-6.918	**< 0.001**
bw28 - bw31	-0.069	0.024	569.653	-0.139	0.000	-2.852	0.051
bw28 - bw35	-0.058	0.024	570.338	-0.128	0.011	-2.390	0.161
bw28 - bw39	-0.089	0.024	571.492	-0.159	-0.019	-3.639	**0.004**
bw28 - bw44	-0.090	0.024	569.612	-0.160	-0.021	-3.712	**0.003**
bw31 - bw35	0.011	0.024	569.262	-0.058	0.081	0.460	0.997
bw31 - bw39	-0.019	0.025	574.211	-0.089	0.051	-0.791	0.969
bw31 - bw44	-0.021	0.024	571.155	-0.091	0.049	-0.858	0.956
bw35 - bw39	-0.031	0.025	575.985	-0.101	0.040	-1.245	0.814
bw35 - bw44	-0.032	0.024	572.350	-0.102	0.038	-1.315	0.777
bw39 - bw44	-0.002	0.024	569.833	-0.071	0.068	-0.064	1.000

Table S9c. Independent contrasts for optomotor response observed in polarization-selected and control female guppies at rotating stimulus of several band widths.

contrast	*stimulus*	*estimate*	*SE*	*df*	*lower.CL*	*upper.CL*	*t.ratio*	*p.value*
C - P	bw25	-0.004	0.038	601.455	-0.078	0.070	-0.112	0.911
C - P	bw28	-0.017	0.038	601.441	-0.091	0.057	-0.456	0.649
C - P	bw31	-0.009	0.038	601.422	-0.083	0.064	-0.247	0.805
C - P	bw35	-0.035	0.038	601.457	-0.109	0.039	-0.938	0.349
C - P	bw39	0.027	0.038	601.458	-0.047	0.101	0.722	0.471
C - P	bw44	-0.013	0.038	601.452	-0.086	0.061	-0.340	0.734

Table S10a. Statistical tests for comparisons in visual temporal resolution between polarization-selected and control female guppies.

Speed deviation from stimulus rotation					
Predictors	*Estimates*	*CI*	*Statistic*	*p*	*df*
(Intercept)	8.38	3.23 – 13.53	5.31	**0.014**	2.87
Selection [P]	-0.46	-8.74 – 7.83	-0.19	0.863	2.64
Speed [24]	-5.93	-7.71 – -4.15	-6.54	**< 0.001**	4398.86
Speed [36]	-23.39	-25.17 – -21.61	-25.78	**< 0.001**	4398.86
Speed [45]	-49.74	-51.52 – -47.96	-54.79	**< 0.001**	4398.84
Rotation[Counterclockwise]	-7.11	-8.36 – -5.85	-11.08	**< 0.001**	4398.89
Selection [P] * Speed [24]	0.31	-2.17 – 2.79	0.25	0.805	4398.91
Selection [P] * Speed [36]	1.26	-1.22 – 3.74	0.99	0.320	4398.91
Selection [P] * Speed [45]	-0.48	-2.96 – 1.99	-0.38	0.701	4398.84
Selection [P] * Rotation[Counterclockwise]	1.29	-0.47 – 3.04	1.44	0.150	4398.98

Proportion of time following the stimulus					
Predictors	*Estimates*	*CI*	*Statistic*	*p*	*df*
(Intercept)	0.87	0.80 – 0.94	39.43	**< 0.001**	3.12
Selection [P]	0.00	-0.14 – 0.15	0.10	0.928	2.52
Speed [24]	0.03	0.00 – 0.06	2.03	**< 0.001**	4398.95
Speed [36]	0.03	-0.00 – 0.05	1.83	0.067	4398.95
Speed [45]	-0.04	-0.06 – -0.01	-2.55	**0.018**	4398.92
Rotation[Counterclockwise]	-0.07	-0.09 – -0.05	-7.33	**< 0.001**	4398.98
Selection [P] * Speed [24]	0.01	-0.02 – 0.04	0.74	0.457	4399.06
Selection [P] * Speed [36]	-0.00	-0.04 – 0.03	-0.20	0.843	4398.99
Selection [P] * Speed [45]	-0.00	-0.04 – 0.04	-0.15	0.884	4398.99

Selection [P] * Rotation[Counterclockwise]	-0.01	-0.05 – 0.03	-0.62	0.536	4398.92

Table S10b. Independent contrasts for speed deviation to stimulus rotation observed in polarization-selected and control females at multiple rotation speeds in clockwise and counterclockwise directions

Selection	*Speed*	*Rotation*	*emmean*	*SE*	*df*	*lower.CL*	*upper.CL*	*t.ratio*	*p.value*
C	14.4	Clockwise	8.379	1.577	2.874	3.233	13.526	5.313	**0.015**
P	14.4	Clockwise	7.922	1.938	2.485	0.966	14.879	4.089	**0.038**
C	24	Clockwise	2.447	1.577	2.872	-2.701	7.594	1.552	0.222
P	24	Clockwise	2.303	1.938	2.488	-4.650	9.256	1.188	0.336
C	36	Clockwise	-15.012	1.577	2.872	-20.160	-9.865	-9.520	**0.003**
P	36	Clockwise	-14.212	1.938	2.488	-21.164	-7.259	-7.332	**0.010**
C	45	Clockwise	-41.357	1.577	2.874	-46.503	-36.210	-26.223	**< 0.001**
P	45	Clockwise	-42.299	1.938	2.485	-49.255	-35.342	-21.830	**0.001**
C	14.4	Counterclockwise	1.272	1.577	2.873	-3.875	6.420	0.807	0.481
P	14.4	Counterclockwise	2.103	1.938	2.487	-4.850	9.057	1.085	0.372
C	24	Counterclockwise	-4.660	1.577	2.869	-9.809	0.489	-2.956	0.063
P	24	Counterclockwise	-3.517	1.939	2.491	-10.465	3.432	-1.814	0.186
C	36	Counterclockwise	-0.483	-22.119	1.577	2.869	-27.268	-14.030	**0.001**
P	36	Counterclockwise	-20.031	1.939	2.491	-26.979	-13.083	-10.331	**0.004**
C	45	Counterclockwise	-48.464	1.577	2.873	-53.611	-43.317	-30.731	**< 0.001**
P	45	Counterclockwise	-48.118	1.938	2.487	-55.071	-41.164	-24.827	**< 0.001**

Table S11. Statistical results using a robust linear mixed model approach for comparisons in the proportion of time following the correct direction of the stimulus in visual temporal assays between polarization-selected and control female guppies.

Proportion of time following the stimulus					
Predictors	*Estimates*	*Std. Error*	*t-value*	*p*	*df*
(Intercept)	0.91	0.016	57.45	**< 0.001**	3.12
Selection [P]	-0.001	0.031	-0.04	0.971	2.52
Speed [24]	0.014	0.009	1.61	0.106	4398.95
Speed [36]	0.027	0.009	3.07	**0.001**	4398.95
Speed [45]	-0.010	0.009	-1.17	0**.240**	4398.92
Rotation[Counterclockwise]	-0.041	0.006	-6.51	**< 0.001**	4398.98
Selection [P] * Speed [24]	0.004	0.012	0.33	0.744	4399.06
Selection [P] * Speed [36]	0.004	0.012	0.33	0.741	4398.99
Selection [P] * Speed [45]	-0.009	0.012	-0.74	0.460	4398.99
Selection [P] * Rotation[Counterclockwise]	-0.001	0.009	-0.15	0.882	4398.92

Robustness weights for the residuals:
3546 weights are ~= 1. The remaining 974 ones are summarized as
Min. 1st Qu. Median Mean 3rd Qu. Max.
0.199 0.328 0.518 0.557 0.773 0.999

Robustness weights for the random effects:
101 weights are ~= 1. The remaining 18 ones are summarized as
Min. 1st Qu. Median Mean 3rd Qu. Max.
0.247 0.489 0.739 0.693 0.904 0.995

Rho functions used for fitting:
Residuals:
eff: smoothed Huber (k = 1.345, s = 10), sig: smoothed Huber, Proposal II (k = 1.345, s = 10)
Random Effects, variance component 1 (trial):
eff: smoothed Huber (k = 1.345, s = 10), vcp: smoothed Huber, Proposal II (k = 1.345, s = 10)
Random Effects, variance component 2 (rep):
eff: smoothed Huber (k = 1.345, s = 10), vcp: smoothed Huber (k = 1.345, s = 10)

R syntax for final models used in statistical analyses

Shoaling patterns (Table S1 + Table S2)

- Polarization_model = lmer(polarization ~ selection line * treatment + body size + (selection line | replicate) + (1 | trial id))
  emmeans(Polarization_model, pairwise ~ line | treatment)

- Activity_model = lmer(median speed ~ selection line * treatment + body size + (selection line | replicate) + (1 | trial id))
  emmeans(Activity_model, pairwise ~ line | treatment)

- Speed_model =lmer(nearest neighbor distance ~ selection line * treatment + body size + (selection line | replicate) + (1 | trial id))
  emmeans(Speed_model, pairwise ~ line | treatment)

Predator inspection behavior (Table S3)

- Number_of_inspections = glmmTMB(inspections ~ selection line + (1 | selection line:replicate) + (1 | Order of stimulus), poisson(link = "log"))

- Total time inspecting = glmmTMB(time inspecting ~ selection line + (1 | selection line:replicate) + (1 | Order of stimulus), genpois(link = "log"))

- Mean inspection duration = glmmTMB(mean inspection ~ selection line + (1 | selection line:replicate) + (1 | Order of stimulus), genpois(link = "log"))

Shoaling patterns during predator inspection trials (Tables S4 + S5)

- Polarization_closer_200mm = lmer(polarization ~ selection line * group position + replicate + (1 | trial id) + (1 | Order of stimulus))
  emmeans(Polarization_closer_200mm, pairwise ~ selection line | group position)

- Polarization_in_tail_head_areas = lmer(polarization ~ selection line * group position + (selection line | replicate) + (1 | trial id) + (1 | Order of stimulus))

emmeans(Polarization_in_tail_head_areas, pairwise ~ selection line | group position

Brain anatomy (Independent Linear Mixed Models for brain regions and whole brain size ; Table S6)

- Whole_brain = lmer(log(brain) ~ selection line + log(standard lentgh) + (1 | replicate))

- Brain_region = lmer(log(brain region) ~ selection line + log(rest of the brain) + (1 | replicate)

Brain anatomy (Multilevel Model for all brain regions; Table S7)

DT = bf(scale(DT) ~ selection line + scale(rest of the brain) + (1 | replicate))
VT = bf(scale(VT) ~ selection line + scale(rest of the brain) + (1 | replicate))
OB = bf(scale(OB) ~ selection line + scale(rest of the brain) + (1 | replicate))
Hyp = bf(scale(Hyp) ~ selection line + scale(rest of the brain) + (1 | replicate))
OT = bf(scale(OT) ~ selection line + scale(rest of the brain) + (1 | replicate))
OTc = bf(scale(OTc) ~ selection line + scale(rest of the brain) + (1 | replicate))
Th = bf(scale(Th) ~ selection line + scale(rest of the brain) + (1 | replicate))
TS = bf(scale(TS) ~ selection line + scale(rest of the brain) + (1 | replicate))
NG = bf(scale(NG) ~ selection line + scale(rest of the brain) + (1 | replicate))
Cb = bf(scale(Cb) ~ selection line + scale(rest of the brain) + (1 | replicate))
MO = bf(scale(MO) ~ selection line + scale(rest of the brain) + (1 | replicate))

Multilevel_model <- brm(mvbf(DT, VT, OB, Hyp, OT, OTc, Th, TS, NG, Cb, MO) + set_rescor(TRUE), chains = 16, cores = 16, control = list(adapt_delta = 0.995, max_treedepth =15), iter = 3000, warmup = 2000)

Eye morphology (Table S8)

- Eye_size = lmer(eye size ~ selection line + (selection line | replicate))

- Relative_eye_size = lmer(relative eye size ~ selection line + (selection line | replicate))

Visual acuity (Table S9)

- Visual_acuity_model = lmer(optomotor response ~ selection line * stimulus bandwidth + time moving in static + (1| fish id) + (selection line | replicate))

```
Stimulus_bandwidth_contrasts <- emmeans(Visual_acuity_model ~ stimulus bandwidth, type = "response")
pairs(Stimulus_bandwidth_contrasts, adjust="tukey")
```

```
Selection_line_contrasts <- emmeans(Visual_acuity_model, ~selection line | stimulus bandwidth, type = "response")
pairs(Selection_line_contrasts)
```

Temporal resolution (Tables S10 and S11)

```
Deviation_speed_model = lmer(speed deviation ~ selection line+ speed of rotation + direction of rotation + selection line : speed of rotation  + selection line : direction of rotation + (1 | trial id) + (selection line | replicate))
Selection_line_contrasts <- emmeans(Deviation_speed_model, ~ selection line | speed of rotation  * direction of rotation, type = "response", pbkrtest.limit = 4520)
pairs(Selection_line_contrasts)
```

```
Proportion_time_following_model = lmer(proportional time following ~ selection line+ speed of rotation + direction of rotation + selection line : speed of rotation  + selection line : direction of rotation + (1 | trial id) + (selection line | replicate))
Selection_line_contrasts <- emmeans(Proportion_time_following_model, ~ selection line | speed of rotation  * direction of rotation, type = "response", pbkrtest.limit = 4520)
pairs(Selection_line_contrasts)
```

```
Proportion_time_following_robust_model <- rlmer(proportional time following ~ selection line+ speed of rotation + direction of rotation + selection line : speed of rotation + selection line : direction of rotation + (1 | trial id) + (selection line | replicate))
```

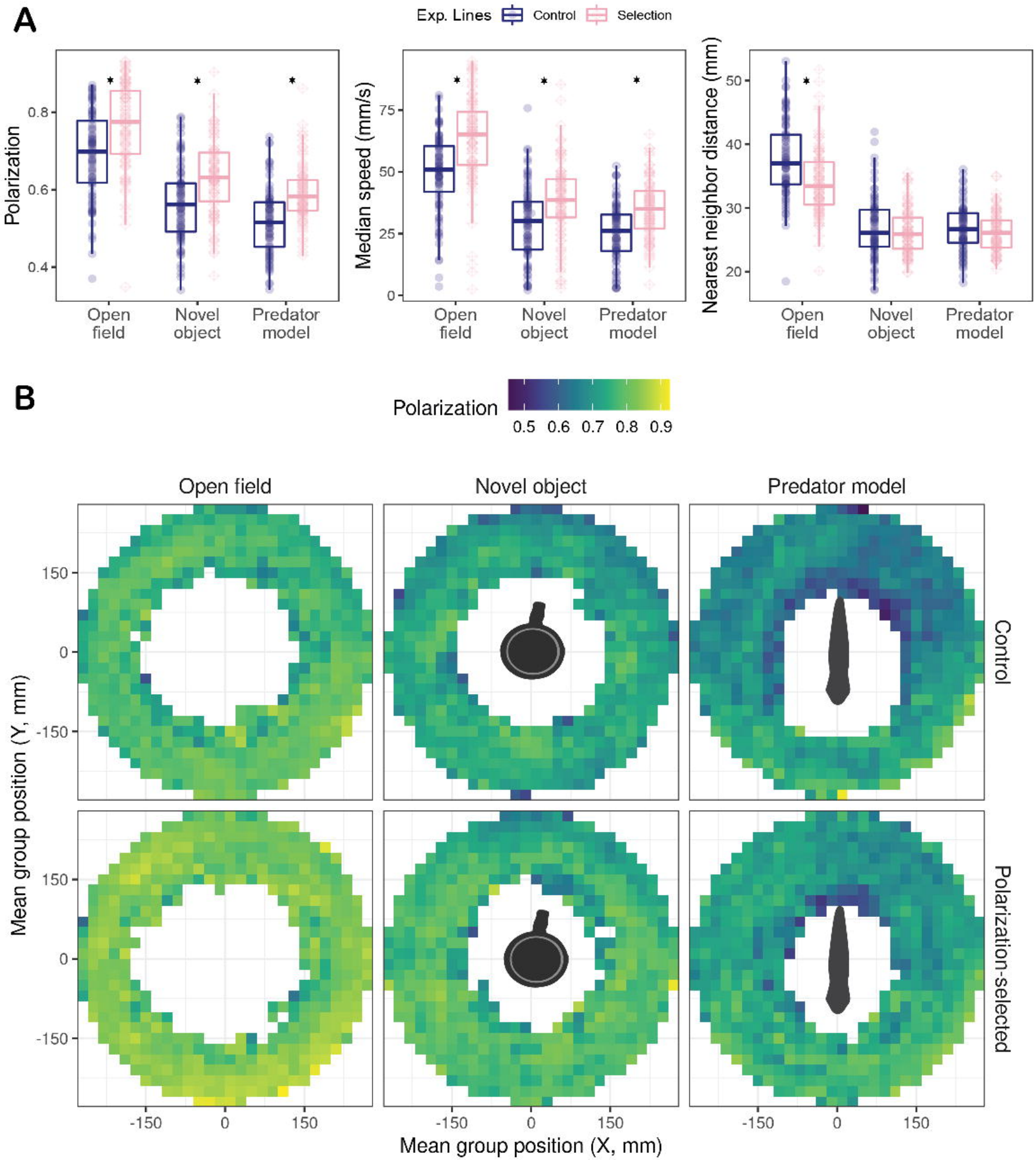
A
Exp. Lines
Control
Selection
Polarization
Median speed (mm/s)
Nearest neighbor distance (mm)
Open field
Novel object
Predator model
B
Polarization
0.5 0.6 0.7 0.8 0.9
Open field
Novel object
Predator model
Control
Polarization-selected
Mean group position (Y, mm)
Mean group position (X, mm)

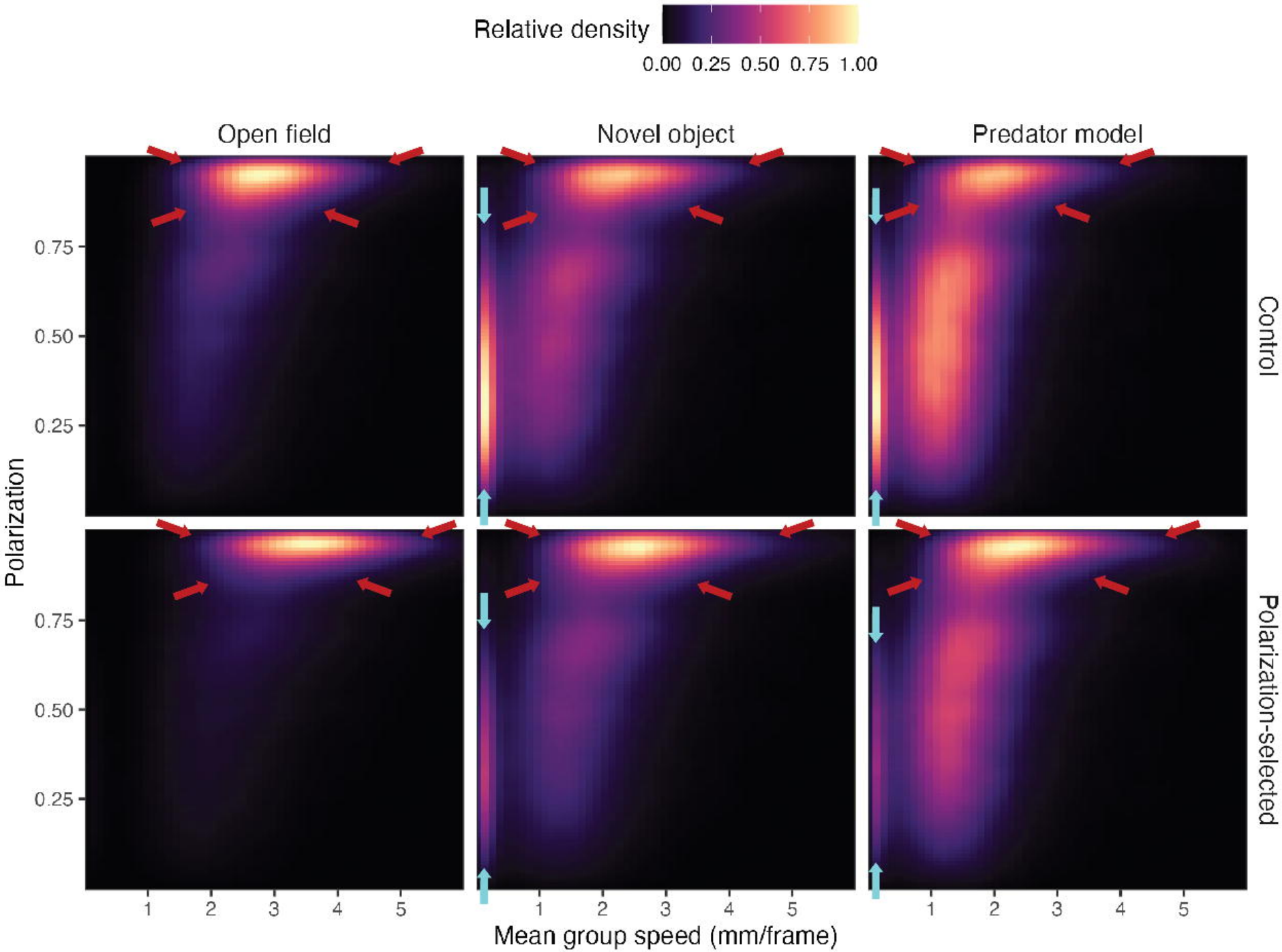
Relative density
0.00 0.25 0.50 0.75 1.00
Open field
Novel object
Predator model
Control
Polarization-selected
Polarization
0.75
0.50
0.25
1 2 3 4 5
Mean group speed (mm/frame)

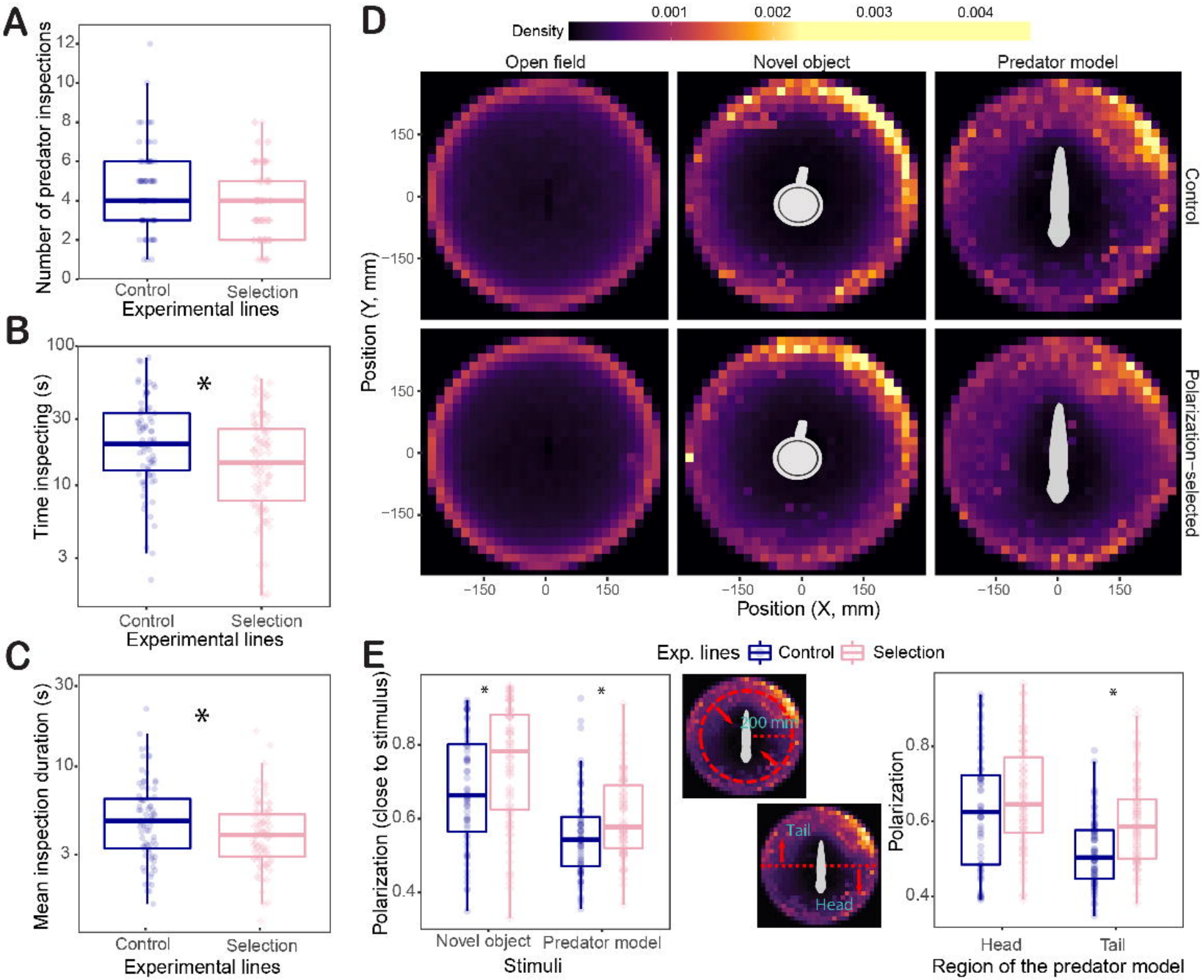
A
Number of predator inspections
Control
Selection
Experimental lines
B
Time inspecting (s)
*
Control
Selection
Experimental lines
C
Mean inspection duration (s)
*
Control
Selection
Experimental lines
D
Density
0.001
0.002
0.003
0.004
Open field
Novel object
Predator model
Control
Polarization−selected
Position (Y, mm)
Position (X, mm)
E
Exp. lines
Control
Selection
Polarization (close to stimulus)
Novel object
Predator model
Stimuli
200 mm
Tail
Head
Polarization
Head
Tail
Region of the predator model

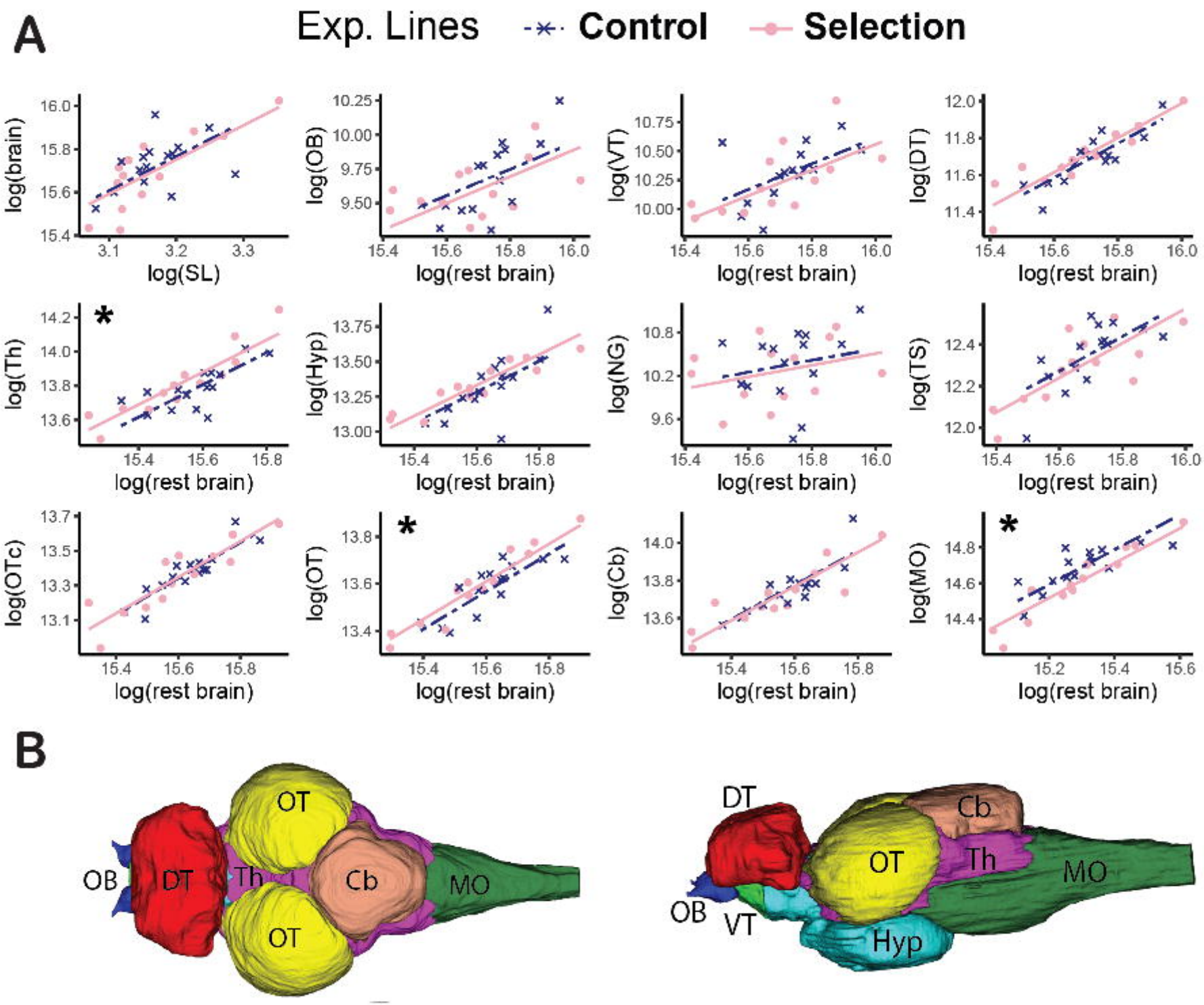
A
Exp. Lines
Control
Selection
log(brain)
log(SL)
log(OB)
log(rest brain)
log(VT)
log(DT)
log(Th)
log(Hyp)
log(NG)
log(TS)
log(OTc)
log(OT)
log(Cb)
log(MO)
*
B
OB
DT
Th
OT
Cb
MO
VT
Hyp

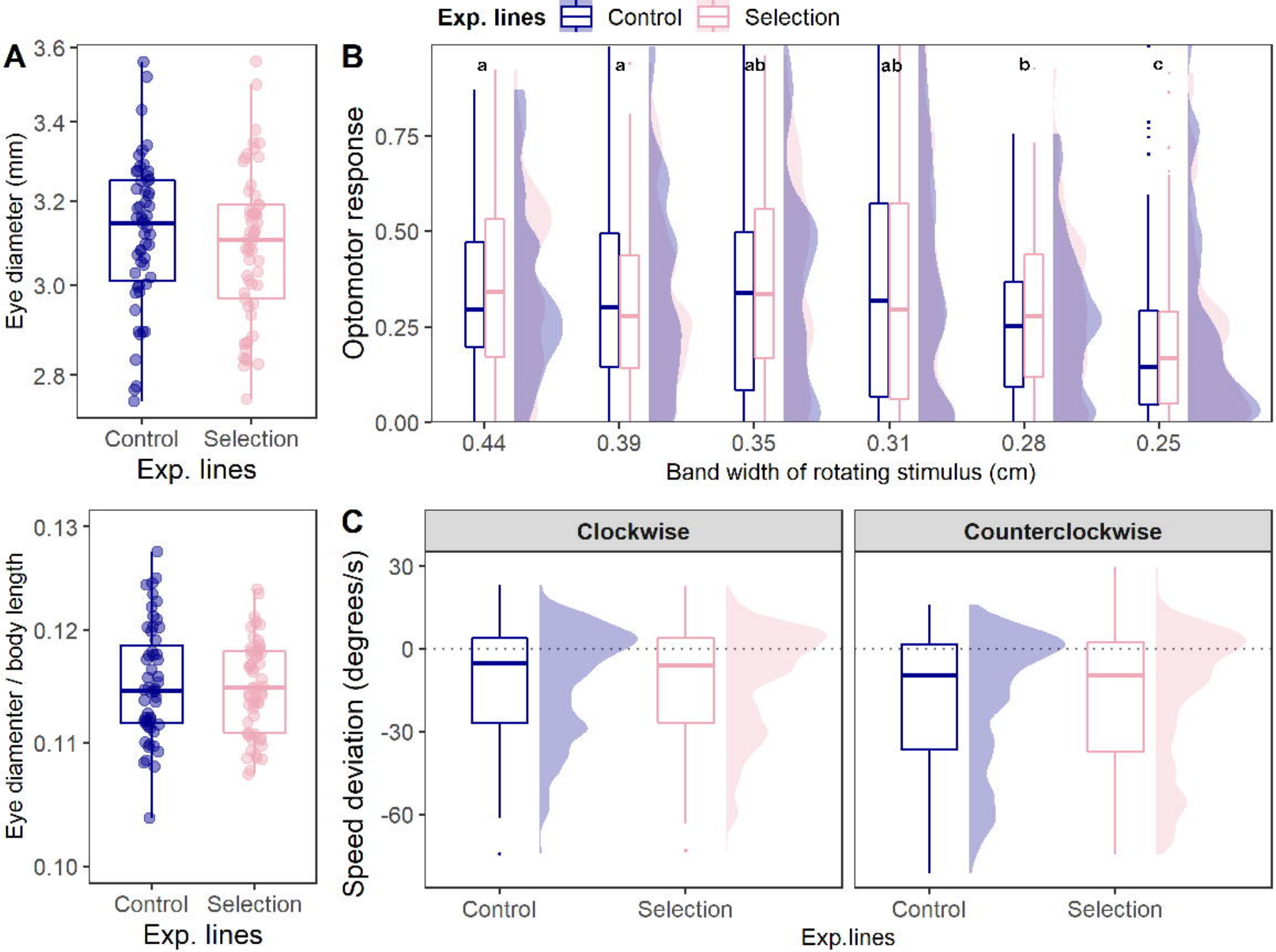
Exp. lines
Control
Selection
A
Eye diameter (mm)
3.6
3.4
3.2
3.0
2.8
Control
Selection
Exp. lines
B
Optomotor response
0.75
0.50
0.25
0.00
a
a
ab
ab
b
c
0.44
0.39
0.35
0.31
0.28
0.25
Band width of rotating stimulus (cm)
Eye diamenter / body length
0.13
0.12
0.11
0.10
Control
Selection
Exp. lines
C
Clockwise
Counterclockwise
Speed deviation (degrees/s)
30
0
-30
-60
Control
Selection
Control
Selection
Exp.lines